Chapter 2. Grain Texture

Introduction

All clastic sediment is made up of discrete particles termed grains or clasts. Thus, any description of a clastic sediment must describe the particles, including their individual and bulk properties. Such properties collectively define the **texture** of a sediment or sedimentary rock and include individual properties such as grain size and shape and bulk properties such as grain size distribution, fabric (orientation and packing of particles), porosity and permeability. These properties are important for any complete description of a sediment. In addition, because these properties are governed by processes that act at the time of deposition and, in some cases, after burial, they might provide insight into the history of a sediment. Furthermore, many of these properties will govern how a sediment will behave when used in a particular way, for example, as a final resting place for garbage. This chapter focuses on the concepts and terminology used to describe sediment texture and shows how texture may be used in making basic interpretations about the history of a sediment.

Grain Size

One might expect that the description of the size of particles that make up a clastic sediment would be the simplest property to describe. However, most sediment is composed of particles with a variety of irregular shapes and may extend over a range of sizes. Therefore, the characterization of the size of particles within a sediment may not be so straight forward.

Consider an irregularly-shaped pebble that is large enough to cover the palm of your hand. How might you tell someone else precisely how big this pebble is without actually showing it to them? You might decide that the pebble is "moderately large" and describe it as such but this is a rather ambiguous expression that could be easily misunderstood by the other person. In this case we need some way of measuring the size of the pebble and then we need some consistent terminology to describe the size; a terminology that everyone else will use so that they will know what is meant by an expression such as "moderately large".

Grain Volume

There are several methods that will provide a quantitative measurement to describe the size of a particle. The easiest method would be to physically measure some linear dimension of a particle. This is simple enough if the particle is a perfect sphere, it will have only one linear dimension: its diameter. However, natural particles are commonly not very spherical and one linear dimension may not adequately describe their size. A measure of size that can be determined while neglecting the shape is the **volume** (V) of a particle. A simple way to determine the volume of a particle is to determine its mass (m) and calculate volume from the relationship:

$$m = V\rho \qquad \text{Eq. 2-1}$$

where ρ is the density of the particle. The mass can be determined by weighing the particle. We might assume a reasonable density of the particle, say that of quartz (2650 kgm^{-3}), and solve for V. However, the actual density of the material comprising the particle may vary significantly from the assumed value.

The volume of the particle may also be determined directly by measuring the volume of fluid displaced by the particle when it is immersed in the fluid within a graduated cylinder or beaker. This method does not require an assumption of the density of the particle but may derive error if the particle is made up of a porous material and all of the pores do not become saturated with the fluid. We can often neglect this source of error.

In the case of particles that are perfect spheres of non-porous solid we can calculate the volume of the particle with diameter *d* from:

$$V = \frac{\pi d^3}{6} \qquad \text{Eq. 2-2}$$

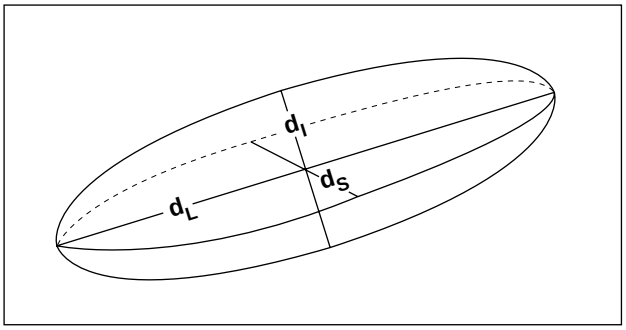

Figure 2-1. Definition of principle axes of a sedimentary particle.

Linear Dimensions

Direct Measurement

As noted above, the easiest way the determine and express the size of a particle is by describing its linear dimensions. Because a sedimentary grain is rarely a perfect sphere we normally treat each grain as if it was a triaxial ellipsoid (Fig. 2-1) and its linear dimensions are described in terms of the lengths of the three principle axes: the long axis (a-axis or d_L), the intermediate axis (b-axis or d_I), and the short axis (c-axis or d_S)

To measure these lengths on a particle follow the steps below and refer to figure 2-2.

1. Determine the plane of maximum projection of the particle. This is an imaginary plane passing through the particle such that the intersection of the particle and the plane produces the largest possible surface area (i.e., the maximum projection area).

2. Establish the maximum tangent rectangle for the maximum projection area. This is a rectangle that, when placed around the maximum projection area, results in the maximum possible tangential contact with the outline of the particle.

3. Measure the length of the a- and b-axes such that the a-axis length is the length of the long side of the maximum tangent rectangle and the b-axis length is the length of the short side of the maximum tangent rectangle.
Note that the plane of maximum projection is the a-b plane of the particle.

4. Measure the c-axis length as the longest distance through the particle, perpendicular to the a-b plane.

The above procedure is used so that different workers can produce comparable results; it provides a standard for all workers. For large particles, reportedly as small as 0.25 mm, all three axes may be measured. For larger particles, in excess of a few millimetres, callipers may be used to measure the axes. For smaller grains the axes may be measured under a binocular microscope. When a grain is too small to allow it to be rotated to see the short axis the long and the intermediate axis may be measured. A common practice is to measure only d_L and different particles may be compared only in terms of their maximum axes lengths. However, this practice may lead to considerable error, especially if the shapes of particles varies considerably.

In many studies of particle size, especially coarse particles, grain size is expressed in terms of the **nominal diameter (d_n)**: *the diameter of a sphere having the same volume as the particle*. If the three principle axes lengths are known this expression of grain size is easily calculated by:

$$d_n = \sqrt[3]{d_L d_I d_S} \qquad \text{Eq. 2-3}$$

Nominal diameter is just one of a large number of expressions of linear dimension that have been used to describe

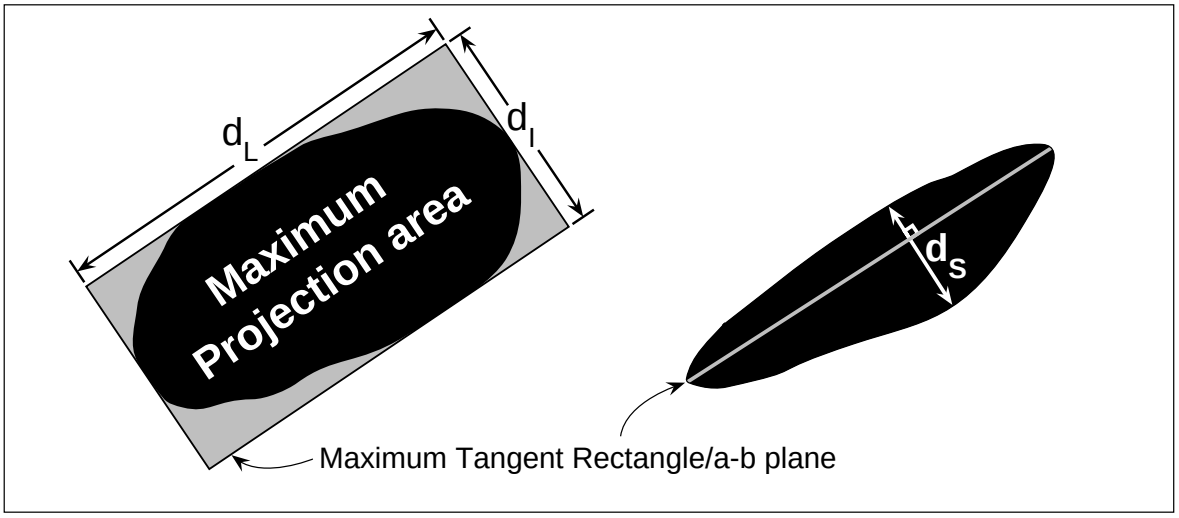

Figure 2-2. Sketch showing the method for determining the lengths of the principle axes of a particle. After Blatt, Middleton and Murray, 1980.

the size of a particle.

Sieving

Sieving is a method that is widely used to directly measure the sizes of a large number of grains (samples range from 40 to 75 grams) and is normally limited to particles in the range from as fine as 0.0625 mm up to as large as 64 mm. The detailed procedure that should be followed when sieving a sediment sample is outlined in Appendix 1. Again, a specific procedure has been derived so that results of different workers will be reliably comparable. The equipment that is used world-wide for sieving includes a shaker and a series of nested, square holed screens (the screen with the largest holes on top, down the smallest holes on the bottom). The sediment sample is passed through the screens, by shaking, and the weight of sediment that accumulates on each screen is weighed. Thus, the information obtained is not the absolute size of each grain but the frequency of grains (by weight), in a sample, that fall between the range of sizes represented by the square holes in the screen above and in the screen on which the grains are resting. The actual dimension of the grains that might be considered is "the largest square hole through which the grains will pass". This dimension is approximately the intermediate axis length. The procedure and the meaning of grain size data will become more clear later in this chapter.

Settling Velocity

Another very useful measure of grain size is the settling velocity of a particle. A particle's settling velocity (or fall velocity) is normally defined as the terminal velocity that a particle will reach while falling through a still fluid, normally water. A particle's settling velocity (ω) is related directly to its size (d) and also to its density (ρ_s) but is also influenced by fluid properties such the fluid density (ρ) and the viscosity (μ); for all fluids these properties vary with temperature.

To measure the settling velocity of a particle we may simply, but accurately, record the time that it takes to fall a known distance through a column of still fluid contained within a transparent tube (termed a settling tube). This is relatively simple if we are timing the settling rate of only one or a few grains but becomes difficult if we must deal with a sample from a population of grains of non-uniform size (and therefore varying settling velocity). In this case we must time the settling rate of large numbers of grains. A variety of types of settling tube have been devised and these are described in several publications (see Blatt *et al.* 1980).

When using settling tubes a number of factors that will influence the results must be considered. First, when

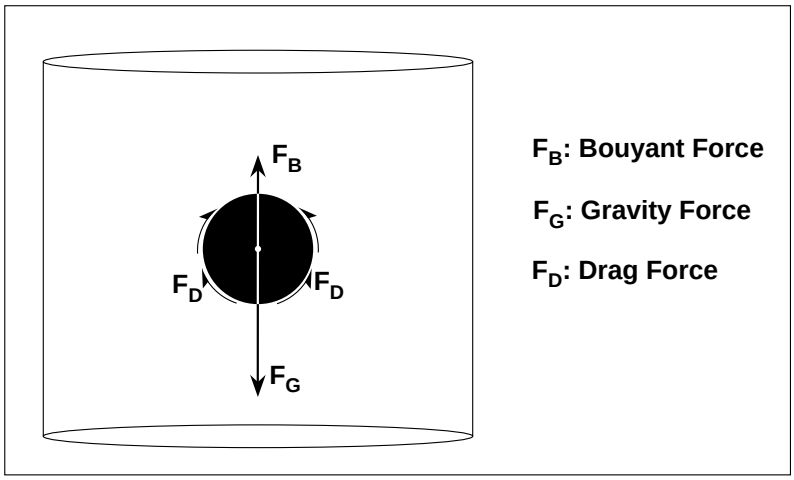

Figure 2-3. Forces acting on a spherical particle falling through a still fluid.

a particle first begins to fall through the fluid it will accelerate from rest (i.e., zero velocity) to some constant (terminal) velocity. Thus, the settling velocity may be under-estimated if the distance over which the particle passes during the phase of acceleration is large in comparison to the total distance over which settling is timed. This can be overcome by using a tube that is long enough so that the distance over which acceleration takes place is relatively small. This may be a problem for relatively large particles but for less than 1 mm diameter particles of quartz-density the distance required to achieve terminal velocity is less than a centimetre. When dealing with samples of more that one particle care must be taken that the grains settle independently and do not interact during passage through the fluid. Sample sizes will depend on the type of settling tube used and should generally be less than 10 grams. Samples that are too large may cause settling *en masse* so that the velocity determined will not be the velocity of individual grains. Also, large quantities of grains in the tube may interact directly (e.g., collide), altering the settling rate, or indirectly by causing the fluid itself to move (i.e., cause turbulence) so that the velocity of the grains is not that in still fluid. A further requirement of apparati for measuring settling velocity is that the tube diameter must be at least five time the average diameter of the particles that will pass through it. When a particle passes through a fluid it must "push" the fluid out of its path. At the tube wall the fluid is more difficult to push than it is well away from the wall region due to fluid viscosity. Thus, a small ratio of tube to particle diameter may result in the passage of grains too close to the tube walls where they will be travel slower than they would through fluid that is not significantly influenced by wall effect.

Stokes' Law of Settling

The relationship between grain size (e.g., diameter) and settling velocity is an interesting one that reflects a variety of principles that will be of interest later in these notes. The relationship is relatively complex due to a number of factors. Theoretical relationships have been developed and compared to experimental data collected by actually measuring settling velocity in settling tubes. One such theoretical relationship between grain size and settling velocity is **Stokes' Law of settling**.

The derivation of Stokes' Law is simple but instructive. It is based on a simple balance of forces that act on a grain as it is falling at terminal velocity through a still fluid and the knowledge that the velocity will be affected by grain size (d), grain density (ρ_s), fluid viscosity (μ), fluid density (ρ), and the acceleration due to gravity (g). Consider the forces acting on the spherical particle falling through a still fluid as shown in figure 2-3. As the particle begins its passage through the fluid three forces are involved: the gravity force (F_G), which is the weight of the particle acting to move it downward through the fluid; a buoyant force (F_B), acting to move the particle upward through the fluid; and a drag force (F_D) that retards the movement of the particle through the fluid. The gravity and buoyant forces may easily be quantified. The gravity force is just the weight of the particle and is equal to the volume of the particle times its density times the acceleration due to gravity:

$$F_G = \frac{\pi}{6}\rho_s g d^3 \qquad \text{Eq. 2-4}$$

F_G acts in the downward direction, causing the particle to settle. The buoyant force acts in the opposite direction and is simply the weight of the fluid that is displaced by the particle (i.e., the weight of fluid with a volume equal to that of the particle):

$$F_B = \frac{\pi}{6}\rho g d^3 \qquad \text{Eq. 2-5}$$

Because F_G and F_B act in opposition the net force that acts on the particle (F_G') is given by:

$$F_G' = F_G - F_B = \frac{\pi}{6}\rho_S g d^3 - \frac{\pi}{6}\rho g d^3 = \frac{\pi}{6}(\rho_S - \rho) g d^3 \qquad \text{Eq. 2-6}$$

Clearly, when the density of the particle exceeds the density of the fluid it will settle through the fluid because $F_G > F_B$. Note that the expression on the right hand side of Eq. 2-6 is termed the *submerged weight* of a particle. The drag force exerted on the settling particle is more difficult to determine. This force arises from the resistance of the fluid to deformation due to the fluid property termed *dynamic viscosity* and is normally given the symbol μ, and is expressed as Nsm^{-2}. Fluids that offer a large resistance to deformation have a high viscosity (e.g. molasses) whereas fluids with low viscosity deform readily. Experiments have shown that the drag on a particle varies with the velocity at which the particle passes through the fluid. Specifically, experiments have shown that at relatively low settling velocities the drag force can be calculated from:

$$F_D = 3\pi d\mu U \qquad \text{Eq. 2-7}$$

Stokes derived his law of settling from the two forces acting on a settling particle: the submerged weight and the drag force. When a particle is settling at its terminal velocity no net force must be acting on it (i.e., the velocity is constant, neither accelerating or decelerating, therefore experiencing no net force). Therefore, when a particle reaches terminal velocity F_D and F_G' must be equal in magnitude but act in opposite directions (F_D acts upwards and the submerged weight acts downwards). Thus, when a particle reaches terminal settling velocity:

$$F_D = F_G - F_B \qquad \text{Eq. 2-8}$$

Setting this equality and substituting with equations 2-6 and 2-7:

$$3\pi d\mu U = \frac{\pi}{6}(\rho_s - \rho) g d^3 \qquad \text{Eq. 2-9}$$

Because the particle is falling at its terminal velocity the velocity term in F_D is the settling velocity so that $U=w$. Therefore, we can solve Eq. 2-9 for ω:

$$\omega = \frac{\pi}{6}(\rho_s - \rho) g d^3 \times \frac{1}{3\pi d\mu} = \frac{(\rho_s - \rho) g d^2}{18\mu} \qquad \text{Eq. 2-10}$$

Thus, Stokes' Law of Settling is simply:

$$\omega = \frac{(\rho_s - \rho) g d^2}{18\mu} \qquad \text{Eq. 2-11}$$

Table 1 shows an example calculation of the settling velocity of a particle using Stokes' Law. Note that when making such a calculation you must state all of the conditions (e.g., sediment and fluid density, fluid temperature and viscosity), in many cases these conditions must be assumed. The statement of conditions is particularly important because there are severe limitations to the use of Stokes' Law of Settling. These limitations are outlined in the following paragraphs.

Stokes' Law is reliable only for grain sizes finer than approximately 0.1 mm. Figure 2-4 shows that Stokes' Law predicts the settling velocity of quartz-density particles quite reliably up to a grain size of approximately 0.1 mm, beyond which the theoretical relationship increasingly overestimates the observed settling velocity. This overestimation is due to the fact that Stokes' Law only includes viscous drag on the particle. When larger grains

Table 2-1. Example of Stokes' Law of Settling

Consider a spherical quartz particle with a diameter of 0.1 mm, in still, distilled water.

ρ_s= 2650 kg/m3

ρ= 998.2 kg/m3, density of water at 20°C

μ = 1.005x10-3 N.s/m2, water at 20°C

g = 9.806 m/s2

(note that in the calculation, for consistent units, the diameter of the particle is expressed as 0.0001 m)

By Stokes' Law the Settling, the terminal fall velocity of this particle is 8.954 x 10-3 m/s (~ 9 mm/s).

settle they travel at relatively high velocities through the fluid and eddies develop in their wake. These eddies impart an additional form of resistance that acts to further reduce their terminal settling velocity. Because Stokes' Law neglects this additional force of resistance it predicts a larger settling velocity than that determined by actual experiments (Fig. 2-4). Figure 2-5 shows an additional shortcoming of Stokes' Law when applied to sedimentary particles that settled in a fluid for which the temperature is not known. Because of the effect of temperature on fluid density and, especially, fluid viscosity, the settling velocity of a particle will vary over almost an order of magnitude through the range of temperatures that might naturally occur at the earth's surface. Thus, application of Stokes' Law to predict the settling velocity of a particle in some unknown depositional environment (and unknown temperature) may lead to considerable error.

A further problem that arises when applying Stokes' Law to natural sedimentary particles is that it only applies to spherical particles. Grain shape can have a dramatic effect on settling velocity. In a simple case, shape can effect the orientation of the grain as it settles thus affecting the surface drag that acts on the particle as it passes through the fluid. A more dramatic example is that of a platy particle (e.g., a flake of mica) which tends to drift back and forth as it settles rather than falling vertically though the fluid.

Finally, Stokes' Law applies to particles falling through a still fluid. That is, the fluid is at rest except where

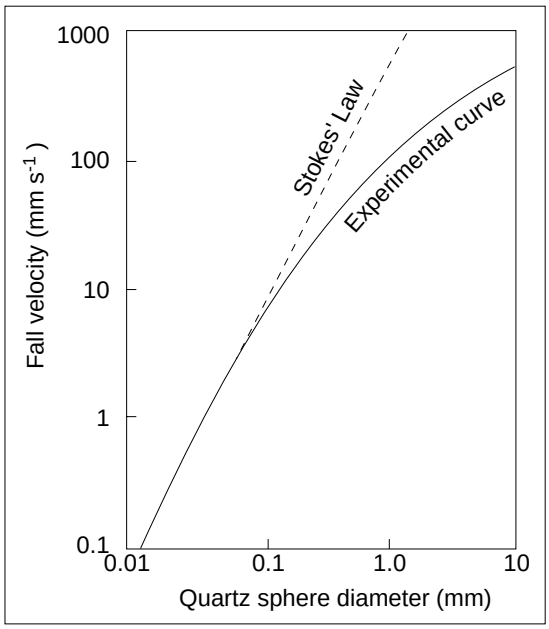

Figure 2-4. Somewhat schematic illustration showing the settling velocities of spherical, quartz-density particles in still water at 20°C, as predicted by Stokes' Law of Settling, compared to experimentally-determined settling velocities of similar particles. After Leeder (1982).

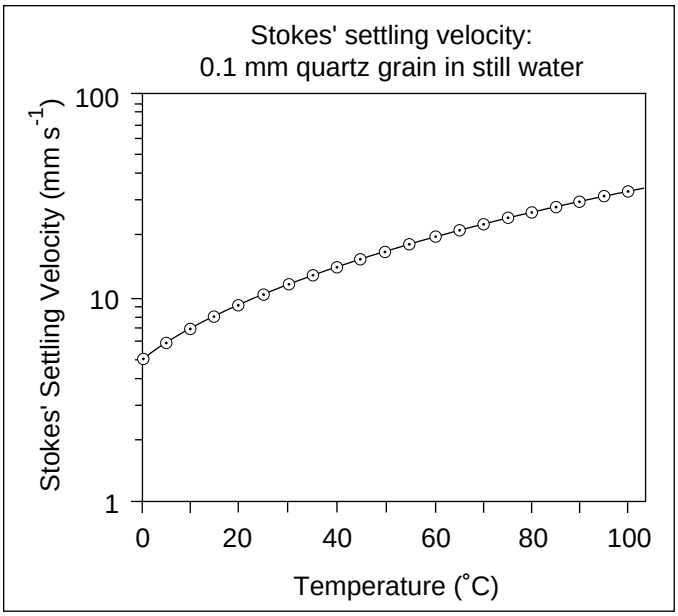

Figure 2-5. Effect of fluid temperature on settling velocity. Curve shows settling velocity calculated using Stokes' Law of Settling applied to a 0.1 mm diameter quartz sphere setting through still water.

it is accelerated, due to viscosity, by the passage of the particle itself. Therefore, it is unreasonable to apply Stokes' Law to the settling velocity of particles in a moving, particularly turbulent, fluid (e.g., particles in a river) where fluid forces will act to move the particle up, down and sideways.

Before leaving Stokes' Law of Settling we can return to the discussion of the expression of grain size as some linear dimension of a particle. Sedimentologists have traditionally preferred to express grain size as some linear dimension and Stokes' Law can also be used to determine such a dimension for comparison of different sedimentary particles. This linear dimension of a particle is termed *Stokes' Diameter* (d_s; also termed settling diameter) of a particle and is defined as *the diameter of a sphere with the same settling velocity as the particle.* We can determine the Stokes' Diameter of a particle by measuring its settling velocity in still water and by solving for particle diameter in Eq. 2-11. Thus, if the settling velocity of a particle is known, Stokes' Diameter may be calculated from:

$$d_s = \sqrt{\frac{18\mu\omega}{(\rho_s - \rho)g}} \qquad \text{Eq. 2-12}$$

Grade Scales

In the introduction to this chapter we posed the question of how do we verbally describe the size of a particle in such a manner that would be understood by others. A grade scale provides such a standard for verbally expressing and quantitatively describing grain size. Any good grade scale should:

(i) Define ranges or classes of grain size (*grade* is the size of particles between two points on a scale. e.g., "very fine sand", is a grade between maximum and minimum size limits),

and

(ii) Proportion the grade limits so that they reflect the significance of the differences between grades. For example, the change in size from 1 mm to 2 mm diameter sand is an increase of 100%, however, the change in size from 10 mm to 11 mm is on the order of 10%. Therefore, a grade scale in which grade limits vary by 1 mm would not be useful.

The most widely-used grade scale is the Udden-Wentworth Grade Scale (Fig. 2-6). Note that most of the grade

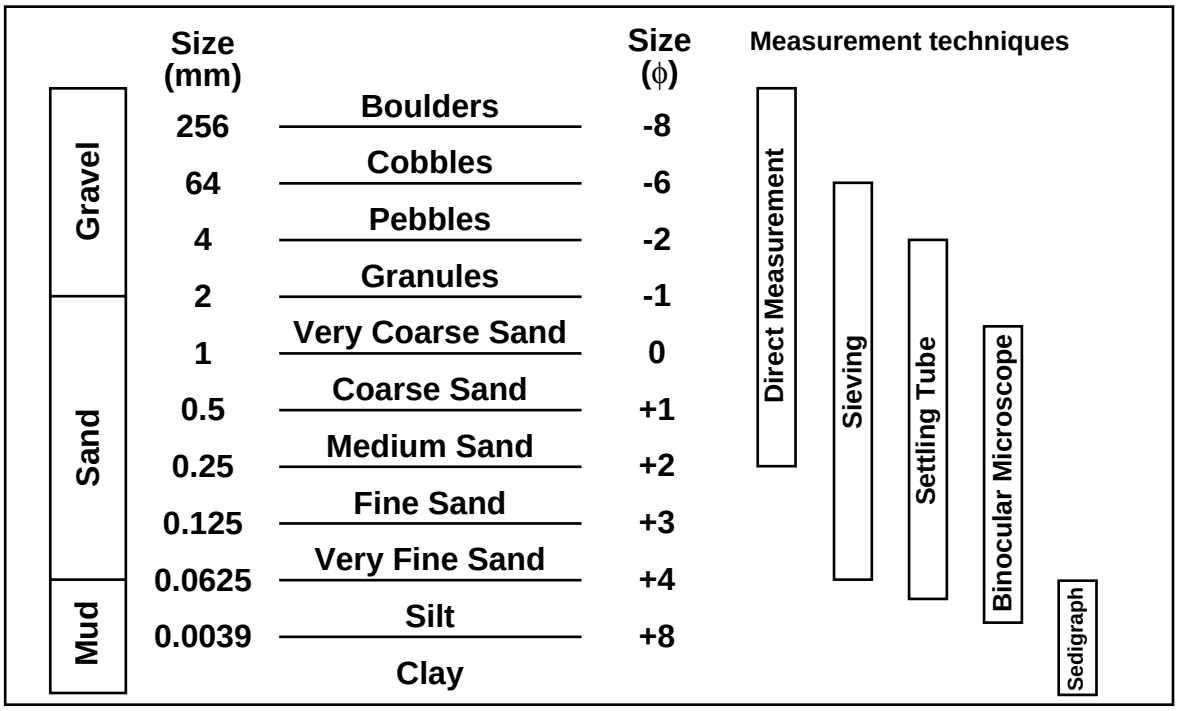

Figure 2-6. The Udden-Wentworth Grade Scale defining the range of sediment sizes per size class and the verbal expression used to describe each size class. Also shown are the techniques that may be used to measure grain size and the grain size limits over which they should be used. After Pettijohn, Potter and Siever, 1973.

boundaries increase by a factor of 2, reflecting significant changes in grain size. Also, the scale defines limits for the verbal expression of grain size. "Very fine sand" is sand which ranges in size from 0.0625 mm to 0.125 mm

Krumbein (1934) introduced a logarithmic transformation of the scale which converts the boundaries between grades to whole numbers. This scale is known as the Phi Scale, it's values being denoted by the Greek letter phi (ϕ), where:

$$\phi = -\log_2 d(mm) \qquad \text{Eq. 2-13}$$

where d(mm) is just the grain size expressed in millimetres. For example:

$$-\log_2 1(mm) = 0\,\phi$$
$$-\log_2 1/4(mm) = 2\,\phi$$
$$-\log_2 4(mm) = -2\,\phi$$

ϕ was later redefined:

$$\phi = -\log_2 d/d_o \qquad 2\text{-}14$$

where d is the size in millimetres and d_o is a standard size of 1 mm; division by 1 mm does not alter the value of ϕ but makes it dimensionless.

With a hand calculator the conversion from ϕ to mm and from mm to ϕ is as follows:

$$\phi \rightarrow mm \qquad d(mm) = 2^{-\phi}$$

$$mm \rightarrow \phi \qquad \phi = -(\log_{10} d)/\log_{10} 2$$

Note that it is traditional among sedimentologists to plot grain size on a phi scale with decreasing grain size to the right as shown in figure 2-7.

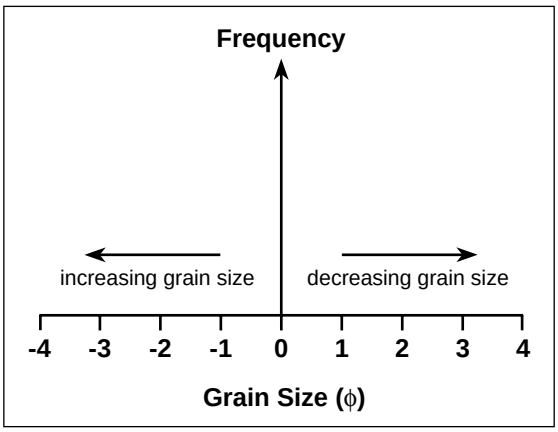

Figure 2-7. Conventional phi scale showing grain size increasing to the left and decreasing to the right.

Displaying Grain Size Data

Most data describing the grain size distribution of a bulk sample of sediment are in the form given in Table 2-2 which shows the frequency distribution (in terms of weight) of sediment per size class (here grain size classes are at 0.5 ϕ intervals). In the case of data derived from sieving a sediment sample each value in column 2 is the weight, in grams, of sediment accumulated on the sieve with openings indicated by the grain size class (column 1). To facilitate comparison of samples of different weight the frequency distribution is more commonly calculated as a weight expressed as a percentage of the total weight of the sample (column 3). Column 4 is the cumulative weight (%) derived by incrementally summing the values in column 3. Several ways in which such data may be plotted to graphically display the grain size distribution of a sample are shown in figure 2-8.

Histograms, such as figure 2-8A, are valuable because they readily show the relative proportions of each size class and the modal class of the distribution (the size class with the largest frequency). Also shown in figure 2-8A is the **frequency curve** for the data, a smoothed version of the histogram formed by joining the midpoints of each size class on the histogram. Note that there are two vertical scales in this example, one shows the absolute weight per size class and the other shows the weight expressed as a percentage of the total sample weight per size class. In this case the data are normally distributed and the frequency curve forms a bell-shape which is symmetrical about its highest point. Figures 2-8B and C are **cumulative frequency curves** for the data in Table 2-2, column 4.

Table 2-2. Example of grain size data produced by sieving (note these data are plotted in Figure 2-8).

1. Grain Size Class (ϕ)	2. Weight (grams)	3. Weight (%)	4. Cumulative Weight (%)
-0.5	0.40	1.3	1.3
0	1.42	4.6	5.9
.5	2.76	8.9	14.8
1	4.92	15.9	30.7
1.5	5.96	19.3	50
2	5.96	19.3	69.3
2.5	4.92	15.9	85.2
3	2.76	8.9	94.1
3.5	1.42	4.6	98.7
4	0.40	1.3	100.0
Total	**30.92**	**100**	

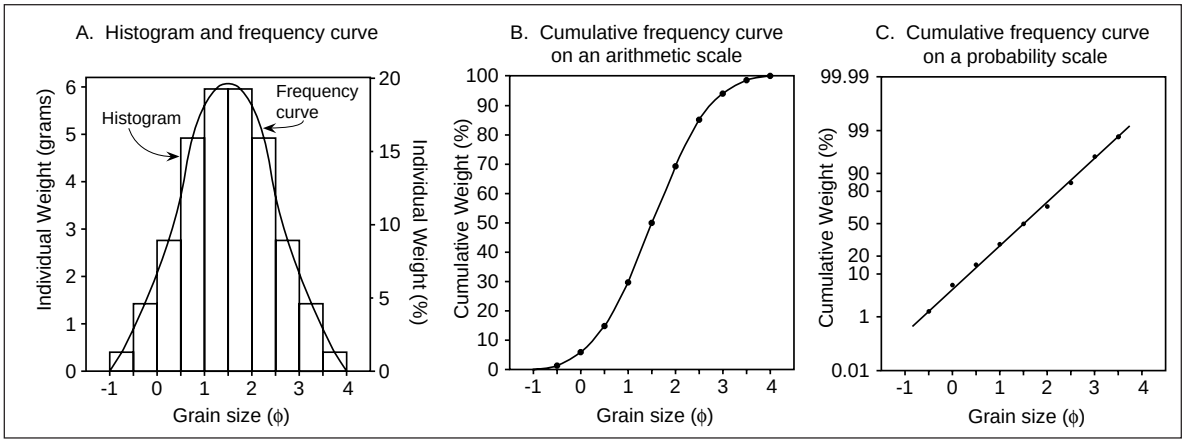

Figure 2-8. Various ways in which grain size data (Table 2-2) may be graphically displayed.

One of the major benefits of plotting grain size data as cumulative frequency curves is that the data form a unique curve for each possible grain size distribution. Such curves may be plotted on graphs with arithmetic axes (Fig. 2-8B) or more commonly on graphs with a vertical "probability" scale which expands the low and high ends of the scale and compresses the middle of the scale (Fig. 2-8C). One advantage of plotting such data on a probability scale (Fig. 2-8C) is that normally-distributed data plot as a straight line. Moreover, if the sediment sample is made up of several normally-distributed subpopulations its' cumulative frequency curve, plotted on a probability scale, will form straight-line segments, each corresponding to a subpopulation of the total sediment (Fig. 2-9B). Another benefit of constructing cumulative frequency curves is that **percentiles** can be taken directly off the graph (Fig. 2-9A). The *n*th percentile (denoted ϕ_n in this context) is the grain size, in units of ϕ, which is finer that *n* % of the total sample. In figure 2-9A ϕ_{20} is shown to be 0.86 ϕfor the hypothetical sample. Several descriptive measures of grain size distributions have been based on percentiles taken directly from cumulative frequency curves (see Table 2-3).

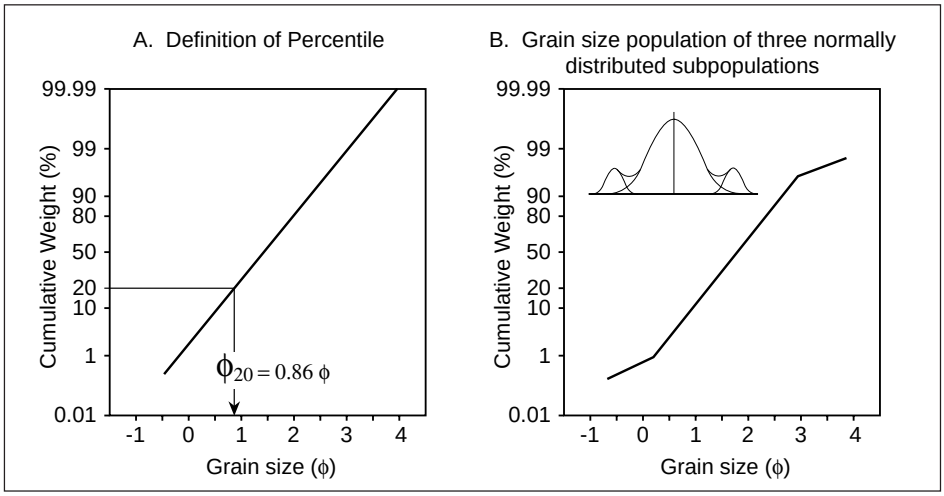

Figure 2-9. A. Illustration showing how a percentile may be determined from a cumulative frequency curve. B. Schematic illustration showing the cumulative frequency curve of a sediment population composed of three subpopulations. Note that both graphs are plotted on probability scales.

Table 2-3. Descriptive measures of sediment size distribution.

Measure	Graphic Method (Folk and Ward, 1957)	Moment Method (after Boggs, 1987)
Median (Md)	ϕ_{50}	–
Mean (M)	$\frac{\phi_{16} + \phi_{50} + \phi_{84}}{3}$	$\frac{\sum fm}{100}$
Standard Deviation (σ)	$\frac{\phi_{84} - \phi_{16}}{4} + \frac{\phi_{95} - \phi_5}{6.6}$	$\sqrt{\frac{\sum f(m-M)^2}{100}}$
Skewness (Sk)	$\frac{\phi_{84} + \phi_{16} - 2\phi_{50}}{2(\phi_{84} - \phi_{16})} + \frac{\phi_{95} + \phi_5 - 2\phi_{50}}{2(\phi_{95} - \phi_5)}$	$\frac{\sum f(m-M)^3}{100\sigma^3}$
Kurtosis (K)	$\frac{\phi_{95} - \phi_5}{2.44(\phi_{75} - \phi_{25})}$	$\frac{\sum f(m-M)^4}{100\sigma^4}$

where: ϕ_n is the *n*th percentile of the size distribution taken from the cumulative frequency curve;
ϕ is the weight of sediment per size class as a percentage of the total sample weight;
m is the midpoint of the size class.

There are several different properties of grain size distributions that may be described both qualitatively and quantitatively. The most common of these are outlined below. Table 2-3 summarizes some widely-used formulae for computing the descriptive measures of grain size distributions. Note that the graphic method uses percentiles taken directly from cumulative frequency curves (see Fig. 2-10)

Median (Md)

This is the mid-point of the distribution (i.e., the grain size for which 50% of the sample is finer and 50% is coarser).

Mean (M)

The mean is the arithmetic average size of the distribution (Fig. 2-11). For perfectly symmetrical normal

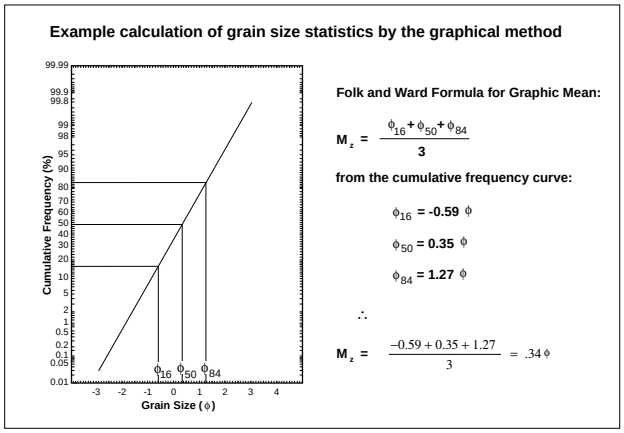

Figure 2-10. Example of calculating the mean of a size distribution by the graphical method.

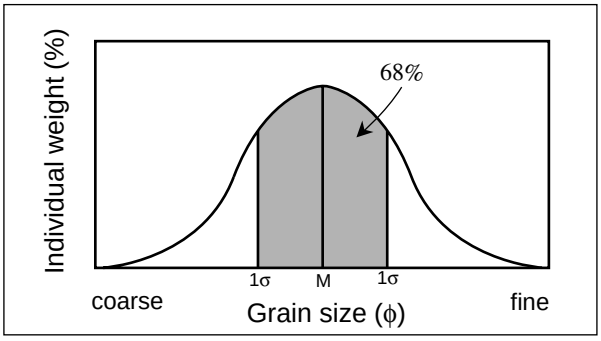

Figure 2-11. Relationship between sorting coefficient (standard deviation) and mean of a normal distribution. After Friedman and Sanders (1978).

distributions the mean is equal to the median. Note that the true mean cannot be determined from data collected by sieving but can be approximated by the formulae shown in Table 2-3.

Sorting or Dispersion Coefficient (σ) (Standard deviation)

This is the standard deviation of the distribution and reflects the variation in grain sizes that make up a sediment. Its' calculated value relates to the mean of the distribution as illustrated in figure 2-11. This figure shows that 68% of the distribution (i.e., 68% of a sediment sample, by weight) has a grain size that is within $\pm 1\sigma$ of the mean. For example, if the mean of the distribution is 1.45 ϕ and the sorting coefficient is 0.30 ϕ, then 68% of the sample lies in the size range from 1.15 ϕ to 1.75 ϕ. Therefore, the larger the sorting coefficient the greater the range of grain sizes that make up the sediment. A sediment that consists of only a small range of grain sizes (i.e., σ is small) is said to be well sorted whereas a sediment made up of a wide range of grain sizes (i.e., σ is large) is said to be poorly sorted. Figure 2-12 very schematically illustrates the appearance of various degrees of sorting. Descriptive grades of sorting are:

$0 < \sigma < 0.35\phi$	very well sorted
$0.35 < \sigma < 0.5\phi$	well sorted
$0.5 < \sigma < 0.71\phi$	moderately well sorted
$0.71 < \sigma < 1.00\phi$	moderately sorted
$1.00 < \sigma < 2.00\phi$	poorly sorted
$2.00 < \sigma < 4.00\phi$	very poorly sorted
$\sigma > 4.00\phi$	extremely poorly sorted

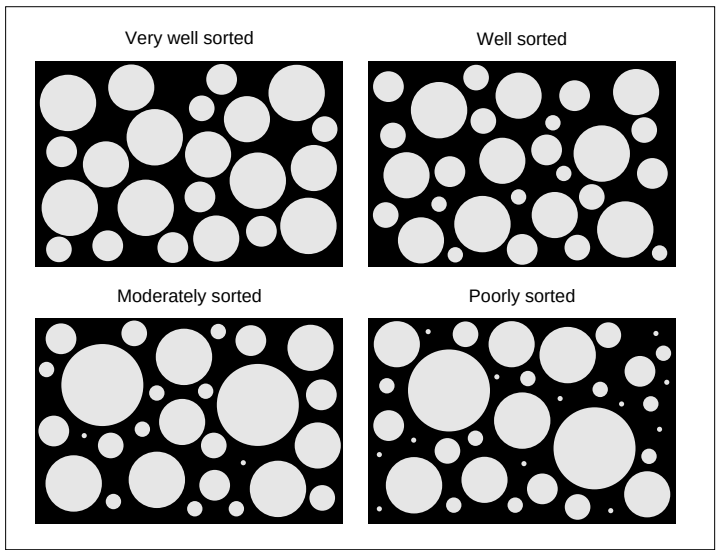

Figure 2-12. Schematic illustration of various degrees of sorting. After Anstey and Chase, 1974.

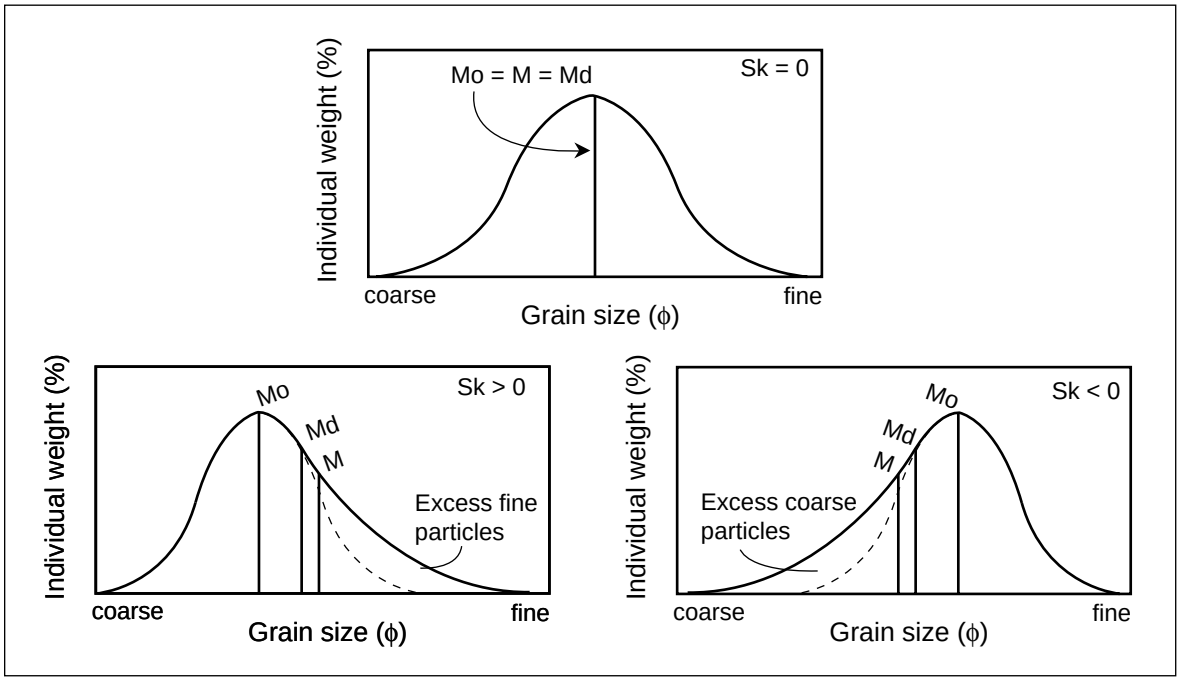

Figure 2-13. Schematic illustration of the various types of skewness. Note that dashed lines indicate the symmetrical distribution for comparison with fine and coarse skewed frequency curves. M is mean, Md is median and Mo is mode.After Friedman and Sanders (1978).

Skewness (Sk)

Skewness is a measure of the symmetry of the grain size distribution about the mean; it has a maximum possible value of +1 and a minimum possible value of -1. A of skewness that is close to zero indicates that the distribution is very symmetrical and the mean is equal, or nearly so, to the median and both fall within the modal class. A positive value of skewness indicates that the distribution has a larger proportion of fine grains than if the distribution were symmetrical. Conversely, if the value of skewness is negative the distribution is enriched in coarse grains. Figure 2-13 schematically shows the various "types" of skewness.

Descriptive terms for skewness are:	Sk > +0.3	strongly fine skewed
	+0.1 < Sk < +0.3	fine skewed
	-0.1 < Sk < +0.1	near symmetrical
	-0.3 < Sk < -0.1	coarse skewed
	Sk < -0.3	strongly coarse skewed

Kurtosis (K)

Kurtosis is a measure of the degree of "peakedness" of the distribution. Oddly enough, while it is one of the common descriptive parameters for grain size distributions it is widely thought to be essentially of no value (see just about any textbook). None-the-less, it has become somewhat of a tradition. Figure 2-14 schematically shows differences between the three types of kurtosis that a distribution might display: leptokurtic (sharp-peaked; K > 1), mesokurtic (normal; K = 1), and platykurtic (flat-peaked; K < 1).

Paleoenvironmental Implications of Grain Size

For many years it was thought (and hoped) that the characteristics of grain size distributions were governed largely by processes within the depositional environment. Therefore, properties like mean size, sorting, skewness, etc., would cumulatively reflect these processes and provide a basis for interpreting ancient depositional environments. This was a powerful reason for sedimentologists to study grain size distributions and many did just

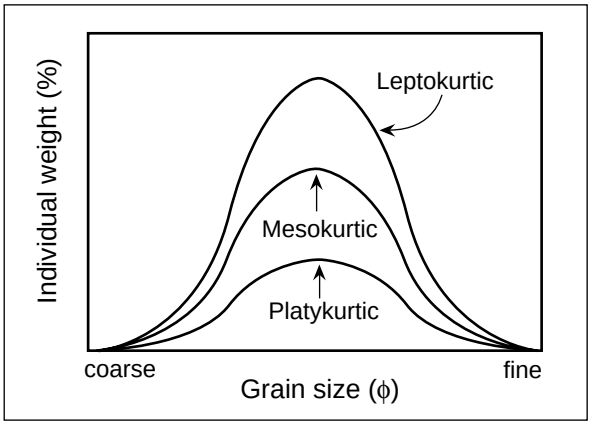

Figure 2-14. Examples of different types of kurtosis. After Blatt, Middleton and Murray (1980).

that throughout much of the 20th century. There was limited success. Results of one successful study are shown in figure 2-15 and suggest that beach and river sediment can be distinguished on the basis of a simple plot of skewness versus standard deviation (sorting coefficient). This figure shows relatively good separation of beach sands (generally coarse skewed and better sorted) and river sands (fine-skewed and somewhat less well sorted). The difference arises because rivers are capable of transporting a relatively wide range of grains sizes, particularly a large proportion of fine sediment that is transported in suspension when the rivers are in flood. The river deposits, therefore, tend to be relatively poorly sorted and enriched in fine grained sand (i.e., fine skewed). In contrast, beaches experience the ongoing swash and backwash of waves running up and down the beach slope. These very shallow flows tend to segregate the sediment very efficiently, particularly in washing fine-grained material out to the sea or lake. Thus, beach deposits are rather well-sorted and somewhat enriched in the coarser grain size (i.e., coarse skewed)

The success of this approach to paleoenvironmental interpretation has been very limited. The main problem is that factors other than processes in the depositional environment have a profound affect on grain size distributions. For example, the size distribution of the constituents of the source rock (i.e., the rock that weathers to produce the sediment) may be reflected in the size distribution of the deposited sediment. If a river is transporting sand that has weathered out of a pre-existing rock formed of sand that was laid down millions of years ago on a beach, the river sediment will continue to display a size distribution which is inherited form the beach deposits.

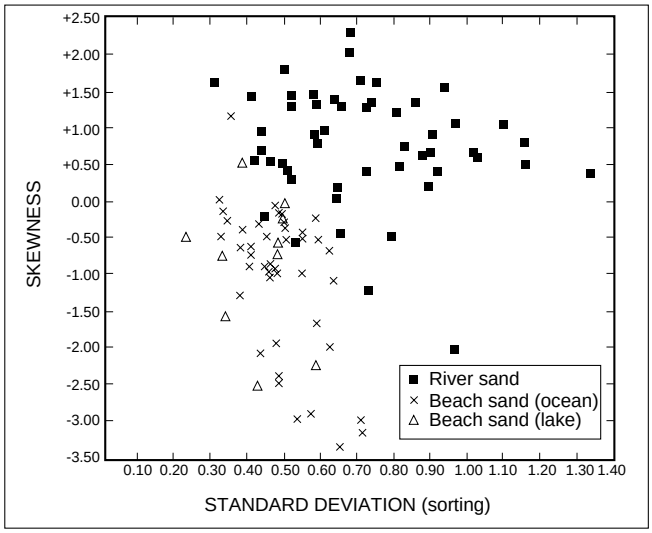

Figure 2-15. Plot of skewness versus sorting coefficient based on samples of river and beach sands. After Friedman, 1967.

Thus, if we plotted that river's sediment on figure 2-15 we would mistakenly interpret the deposit as that of a beach.

Why measure grain size?

There are many reasons to quantitatively describe grain size distributions. Some of these are:

1. Grain size is important to determining the strength of currents that transported the sediment. Therefore, we need a precise measurement of size to quantitatively interpret paleohydraulic conditions.

2. Sorting reflects the ability of the transport mechanism to segregate grains by size.

3. Skewness reflects the ability of the transport mechanism to **selectively** remove coarse or fine grain sizes.

4. It appears that grain size distributions like that shown in figure 2-9B have very specific interpretations in terms of how the sediment moved while it was in transport. (More on points 1 through 4 later in Chapter 4.)

5. We need basic descriptors of sediment size to allow us to communicate with others.

6. Grain size and various properties of its distribution are important in determining a sediment's porosity and permeability.

GRAIN SHAPE

Grain shape is another fundamental property of particles and one that may provide important information about the history of a sediment. Like grain size, shape may be expressed in several different ways, including: *Roundness*, a measure of the sharpness of the corners of a grain; *Sphericity*, a measure of the degree of similarity between a grain and a perfect sphere; *Form*, an expression of the overall appearance of a particle. Methods of quantitatively describing these three expressions of grain shape are outlined below.

Roundness

The roundness of a particle refers to the degree of rounding (or angularity) of the edges of a particle. Of the three shape properties it is the most difficult to quantify.

Wadell's Roundness (R_w)

Wadell (1932) introduced this method of determining particle roundness; it is the most accurate method but it involves the greatest effort and time. R_w is defined as *the ratio of the average radii of curvature of the corners of a grain* ($\Sigma r/N$; *N is the number of corners) to the radius of the largest inscribed circle within the particle* (R; Fig. 2-16). The maximum possible value of R_w is 1 when the particle has no measurable corners (i.e., R = r). Thus,

$$R_W = \frac{\sum r}{NR} \qquad \text{Eq. 2-15}$$

Dobkins and Folk Roundness (R_F)

Dobkins and Folk (1970) introduced a less tedious (and less accurate) method of calculating roundness (symbolized as R_F here) that is defined *as the ratio of the radius of curvature of the particle's sharpest corner (r) to the radius of the largest inscribed circle (R).* Thus,

$$R_F = \frac{r}{R} \qquad \text{Eq. 2-16}$$

once again, R_F approaches a value of 1 for perfectly rounded grains (i.e., no sharp corners).

Powers' visual comparison chart

The easiest way to determine the roundness of a particle is by visual comparison with standard forms. Powers

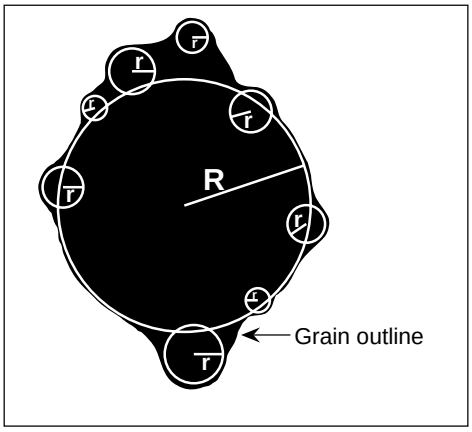

Figure 2-16 Wadell Roundness (see Eq. 2-15; after Boggs, 1967).

(1953) provided what has become the most widely used chart of grain roundness (Fig. 2-17) and is a basis for terms describing roundness. Note that each box in figure 2-17 shows a particular roundness class and the appropriate term to describe each class. Also shown are values of R_w and ρ (a logarithmic transformation of R_w to whole numbers) that quantitatively define the limits of each roundness class.

Sphericity

Various measures of the degree to which a particle resembles a sphere (i.e., its sphericity) have been devised. Sphericity not only describes one aspect of the shape of a particle but it may also be useful to understanding other properties of the particle such as its settling velocity. Remember, Stoke's Law of Settling applies accurately only to spherical particles (less that 0.1 mm in diameter) and its error increases as the shape of the particle deviates from that of a true sphere. Therefore, a measure of particle sphericity provides a means of quantitatively determining how well Stokes' Law will predict a particles' settling velocity. Note that sphericity is normally given the symbol "ψ", the lower case Greek letter psi.

Wadell's Sphericity (ψ)

Wadell (1932) defined sphericity as *the ratio of the diameter of a sphere with volume equal to that of the particle to the diameter of the sphere which will circumscribe the particle*. Wadell's measure of sphericity may take the form:

$$\psi = \sqrt[3]{\frac{V_S}{V_C}} \qquad \text{Eq. 2-17}$$

where V_S is the volume of the sphere with volume equal to that of the particle and V_C is the volume of the circumscribing sphere. In this form V_S may be determined by measuring the volume of water displaced by the particle

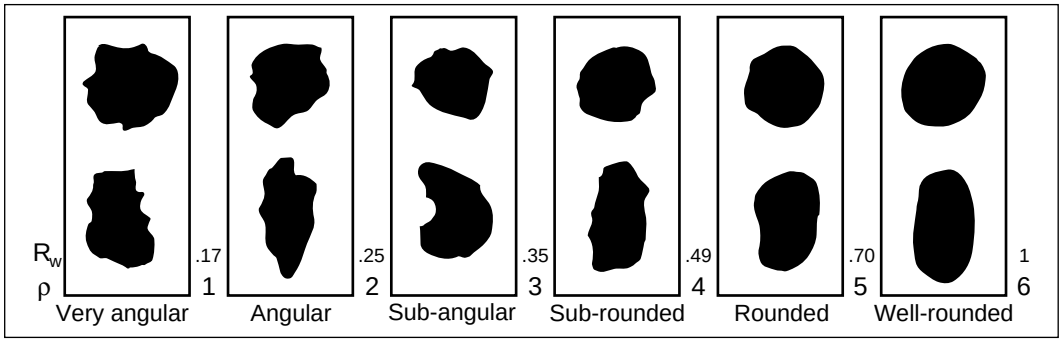

Figure 2-17. Powers' (1953) visual comparison chart for grain roundness with appropriate terms for describing shape classes defined by R_w and ρ.

and V_C may be calculated from the formula for the volume of a sphere taking the maximum axis length of the particle (d_L) to be the diameter of the circumscribing sphere:

$$V_C = \frac{\pi}{6} d_L^3 \qquad \text{Eq. 2-18}$$

V_C may also be calculated for a particle with shaped approximately like a triaxial ellipsoid (Fig. 2-1) by:

$$V_S = \frac{\pi}{6} d_L d_I d_S \qquad \text{Eq. 2-19}$$

Substituting these expressions for Eqs. 2-18 and 2-19 into Eq. 2-17 yields:

$$\psi = \sqrt[3]{\frac{d_I d_s}{d_L^2}} \qquad \text{Eq. 2-20}$$

As ψ approaches 1 the shape of the particle approaches that of a perfect sphere. Eq. 2-20 can be used to calculate sphericity on the basis of measurements of the principle axes of a particle.

Sneed and Folk Sphericity (y_p)

Sneed and Folk (1958) argued that the volume of a particle is not as important as its maximum projection area in determining its settling velocity because drag forces act on the particle's surface. Therefore, any measure of particle sphericity must be reflect the maximum projection area of a particle. They defined **maximum projection sphericity** (ψ_p) as *the ratio of the maximum projection area of a sphere with volume equal to that of the particle to the maximum projection area of the particle*. ψ_p may be calculated from the formula:

$$\psi_P = \sqrt[3]{\frac{d_S^2}{d_L d_I}} \qquad \text{Eq. 2-21}$$

This is the most widely-used expression of sphericity.

Note that an expression that is very similar to ψ_p and based on similar reasoning, termed the Corey Shape Factor (S.F.), is widely by used engineers to describe the overall shape of a sediment particle:

$$S.F. = \frac{d_S}{\sqrt{d_L d_I}} \qquad \text{Eq. 2-22}$$

Riley Sphericity (ψ_R)

The main problem in calculating ψ and ψ_P is that both require the measurement of d_S. This is not difficult for gravel-size particles but it becomes very impractical for sand-size sediment. Riley suggested a method of calculating sphericity that relies on measurements that can be taken from the two-dimensional view of a sand grain as seen through a microscope (Fig. 2-18). He defined an expression of sphericity as:

$$\psi_R = \sqrt{\frac{d_i}{d_c}} \qquad \text{Eq. 2-23}$$

where d_c is the diameter of a circle that circumscribes the grain and d_i is the diameter of a circle that inscribes the grain (Fig. 2-18). Again, as ψ_R approaches unity as sphericity increases.

Clast Form

There are two commonly used methods of describing the overall form of a particle, both based on various ratios of d_L, d_i, and d_S. Figure 2-19 shows the so-called Zingg diagram (after Zingg, 1935) that defines four form fields and provides terms for clast form according to which field the axes ratios of a clast plot. The clast forms defined by the Zingg Diagram are largely independent of sphericity, except for "equant" clasts which tend to have values of sphericity near 1.

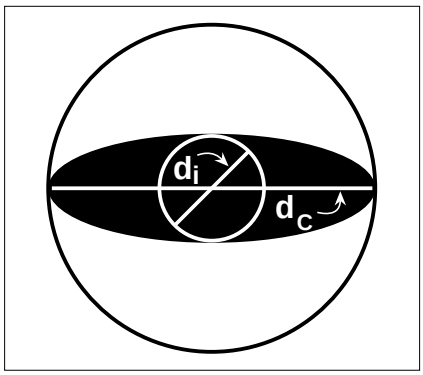

Figure 2-18. Illustration showing the measurements required to calculate sphericity by the method proposed by Riley.

Figure 2-20 shows a second commonly-used scheme for classifying grain form that was proposed by Sneed and Folk (1958). This method classifies form into 10 possible classes and the appropriate terms for each form class is shown in figure 2-20 along with blocks that are drawn in the approximate proportions for each form field. Note also that maximum projection sphericity may also be taken directly from this diagram and that different form classes may have the same sphericity (i.e., form and sphericity are independent).

Significance of grain shape

Like grain size, the shape of a particle will provide some basis for making fundamental interpretations about the "history" of a sediment, particularly something of the source rock of the grains and of their transport history.

Source Rock

The lithology of the source rock exerts a strong control on the form of particles, especially gravel-size clasts. Bedded source rocks (e.g., horizontally bedded limestones) tend to produce platy clasts, due to the parallel planes of weakness that the bedding produces. Massive source rocks (e.g., granites that have equal strength in all directions) tend to produce more equant clasts. The hardness of the source rock will also control the overall shape

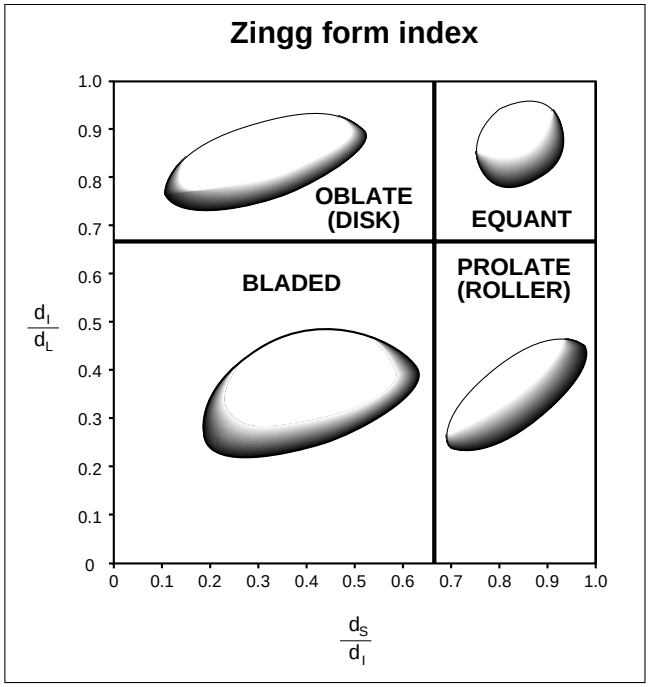

Figure 2-19. Zingg diagram showing the classification of grain form. After Zingg (1935) and Blatt, Middleton and Murray, 1980.

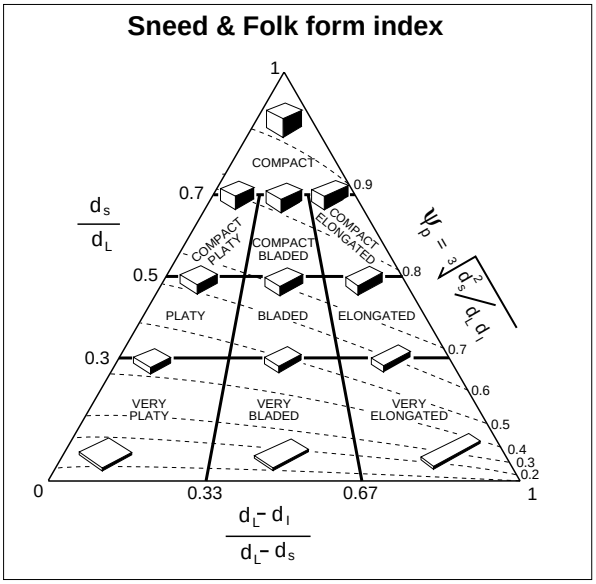

Figure 2-20. Sneed and Folk (1958) classification of grain form.

of a particle, particularly after prolonged periods of transport (see below).

Transport

While in transport a grain will change in shape due to two major processes that may act in the transporting medium. Interaction between grains during transport results in a change in shape and a reduction in grain size. As grains move along their sharp edges are lost due to chipping and grinding, increasing their roundness and sphericity and producing debris as finer sediment. Even when large clasts are partially buried in sediment beneath a current their exposed surfaces are sand-blasted by particles in transport, thereby increasing their overall roundness. However, grains may be crushed during transport, producing smaller, more angular and less spherical grains. Overall, the most common outcome of transport is an increase in roundness and sphericity.

Figure 2-21 shows a plot of data derived by Humbert (1968) from experiments in which angular pebble-size clasts of chert (a very hard rock type) and limestone (relatively soft) were transported over several hundreds of kilometres in a circular flume. Note that the roundness of the limestone increased more rapidly with transport that the chert because the softer limestone clasts are more prone to breakage (which increases rounding) than the harder chert clasts. Also, the rate of increase in rounding with increased transport distance is initially very large but becomes smaller as the grains became rounder. This reflects the fact that an angular clast, with very sharp corners, easily becomes rounder as the fragile corners are broken off. However, a consequence of this increased rounding is that the remaining corners are more massive and difficult to break off. Therefore, as the degree of rounding increases the rate of rounding decreases. The change in the sphericity of limestone clasts shown by the top curve in figure 2-21 is at a comparatively low rate throughout the entire distance of transport. This is because the changes that are required to increase sphericity involve removal of a considerable amount of material from the clasts in contrast to the removal of relatively small sharp corners that results in initially dramatic increases in clast roundness.

Changes in roundness and sphericity with transport of gravel-size clasts occur at much greater rates than for sand-size grains (e.g., Kuenen, 1964). Because little quantitative research on changes in grain shape with transport has been conducted on fine-grained sediment we can infer something of such changes from studies of the weight loss of sand with transport (increased rounding and sphericity both require weight loss). It has been estimated that under water flows (e.g., rivers) the rate of weight loss of quartz grains finer than 2 mm is less than 0.1% per 1000 km of transport. The rate increases only by a factor of two for feldspar grains. In all cases the rate of weight loss decreases sharply with decreasing grain size and becomes negligible for sizes finer than 0.05 mm. Such low rates of weight loss in very fine sediment is largely attributed to the fact that the particles spend much of their time in transport in suspension well above the bed where interaction between particles is less frequent. In

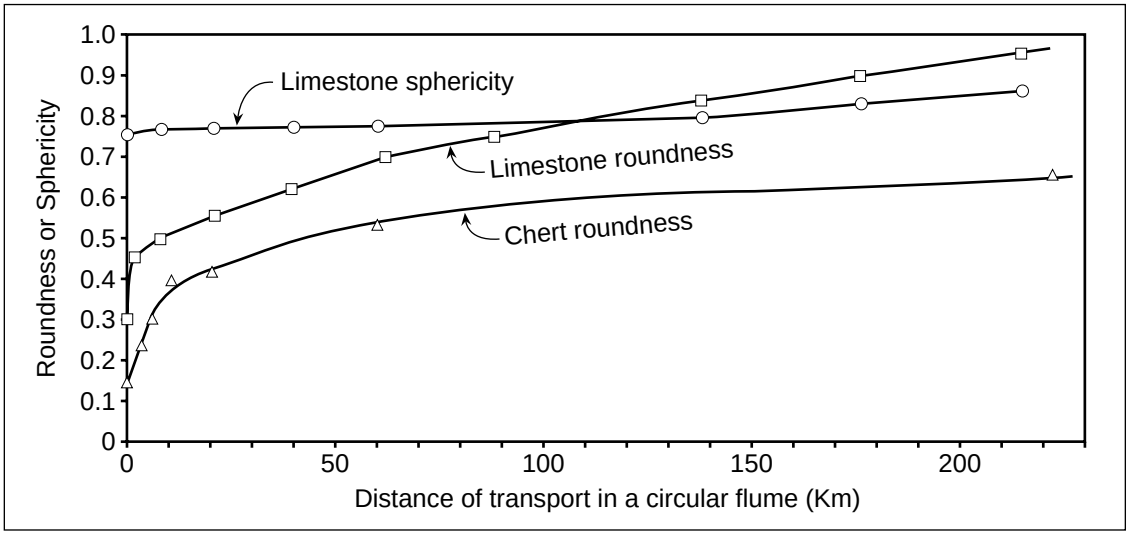

Figure 2-21. Change in rounding (R_w) and sphericity (y_p) with transport distance in a circular flume. Based on experiments by Humbert (1968). After Blatt, Middleton and Murray, 1980.

air the rate of weight loss increases by a factor of 100 to 1000 times the rate in water. In water the abrasion between particles that is required for such weight loss is inhibited by two factors: (1) the small **submerged** weight of the grains gives them only little momentum during collisions, momentum that is required to cause damage; and (2) the viscosity of the water between colliding grains tends to dampen the collisions (further decreasing the transfer of momentum). In air, which has a considerably lower density and viscosity than water, the transfer of momentum between colliding grains is much more effective and the resulting damage to the particles is more extensive. This (partly) explains the common observation that wind-blown (eolian) sands are typically much rounder and have higher values of sphericity than sands from other environments. In ancient sediment that is clearly not of eolian origin good rounding and high sphericity are commonly interpreted to indicate that the sediment has been multi-cycled (i.e., the product of several cycles of weathering and erosion of pre-existing sedimentary rocks).

Transport may have another effect on the shape by selectively sorting clasts by shape. For example, imagine a cube and a sphere resting on the bed of a river. The sphere need only roll almost effortlessly along the bed in response to the fluid drag of the flowing water. In contrast, the cube must pivot over 45°, against its own weight, to roll a distance equal to its own length (if friction between the clast and the bed is large enough to inhibit it from sliding). Thus, the sphere will more readily move under the river's current and after a short time it will be separated from the cube by a considerable distance. This processes is termed **selective sorting** by shape whereby easily transported round, spherical clasts are removed from a sediment much more readily than their angular counterparts, even if both clast types have essentially the same weight. This mechanism has been suggested by studies of some modern river gravels where there is an increase in roundness and sphericity in the downstream direction that cannot be explained solely by abrasion (e.g., Gustavson, 1974).

There has been limited success in distinguishing ancient depositional environments on the basis of clast form. One such study showed that the deposits of gravel beaches and rivers (remember grain size) can be distinguished on the basis of clast form. When data from these environments are plotted as in figure 2-20 the beach gravels tend to fall towards the bottom of the graph, in and about the very platy and very bladed fields, and the river gravels tend to fall near the top of the graph, in and about the compact field. The distinction may be attributed to two causes. First, due to selective sorting of bladed clasts on the beach slope where rounded, compact clasts would be easily rolled off the beach by the backwash (water running back off the beach after a wave has rushed up its slope- the uprush is termed swash). This process would tend to enrich the beach with bladed clasts over time. Second, the swash and backwash act to move larger, less mobile particles up and down the beach slope without

moving them entirely. This back and forth motion would result in abrasion along the basal plane of the clast and as it is periodically flipped over it would become increasingly flat (i.e., bladed or platy). These two mechanisms are absent in rivers where currents can more efficiently roll the more compact particles along their beds.

In conclusion, grain shape is an important sediment property that, like grain size, provides hints as to the processes that acted to transport particles in ancient depositional environments. It is also an important variable in determining the conditions that will cause a sediment to be transported by a specific mechanisms (see chapter 4). However, as with grain size, caution must be used in inferring ancient depositional conditions on the basis of grain shape because it is also controlled by factors other than those acting in the depositional environment.

POROSITY AND PERMEABILITY

Porosity, the proportion of void or pore space in a sediment, and permeability, which is related to how well the voids are connected, are important properties of any sediment or sedimentary rock. This is particularly true because of the possible fluids that might be contained within sedimentary deposits; e.g., water, oil and/or gas, contaminants that humans have added to the earth surface. This section defines and discusses porosity and permeability and shows how they are related.

Porosity

Any sediment contains a certain proportion of void space; that is, the proportion of the sediment that is not occupied by particulate solids (i.e., grains). Porosity (P) is defined as the ratio of void volume (V_p) to total rock or sediment volume (V_T), expressed as a percentage of the total sediment volume. Therefore,

$$P = \frac{V_P}{V_T} \times 100 \qquad \text{Eq. 2-24}$$

The pore volume is generally difficult to measure whereas the total volume of grains in a sediment (V_G) is relatively easy to determine (by weighing a specimen or by placing it in water and measuring the total displacement). Because total volume is the sum of pore and grain volumes V_p can easily be calculated: $V_p = V_T - V_G$. Substituting for V_P in Eq. 2-24, porosity is most commonly defined as:

$$P = \frac{V_T - V_G}{V_T} \times 100 \qquad \text{Eq. 2-25}$$

Porosity in natural sediment varies from 0 to approximately 70% due to a number of factors.

What Controls Porosity?

Packing Density

There are a variety of ways that grains may be arranged in a sediment and the spacing of the particles, referred to as the packing density, exerts a strong control on porosity. This may be very simply illustrated by the manner in which perfect spheres of equal size may be packed (Fig. 2-22). This figure shows the two-dimensional view of spheres resting with cubic and rhombohedral packing. In the case of cubic packing the grains are stacked directly on top of and beside each other and the pore space is relatively large (48% porosity). In contrast, with rhombohedral packing each grain rests in the space between the subjacent grains so that the grains fill more of the space and the porosity is lower (26%). These two styles of packing produce the theoretical maximum (cubic) and minimum (rhombohedral) porosities of any sediment composed of perfectly spherical particles of equal size. In nature, particles may be arranged in styles intermediate to these two end-members and their porosities will also be of an intermediate value (i.e., between 26 and 48%). The rate of deposition of a sediment exerts considerable control over grain packing. Rapidly deposited sands tend to have a more open framework (like cubic packing) whereas slow rates of deposition often lead to tighter packing and therefore lower porosity.

Natural sediment is rarely composed of spheres so that porosity varies over a wider range than predicted above. Porosity varies particularly with grain shape due to the differences in packing density that may be achieved by non-spherical grains. Figure 2-23 shows how much greater porosity may vary when the particles are non-

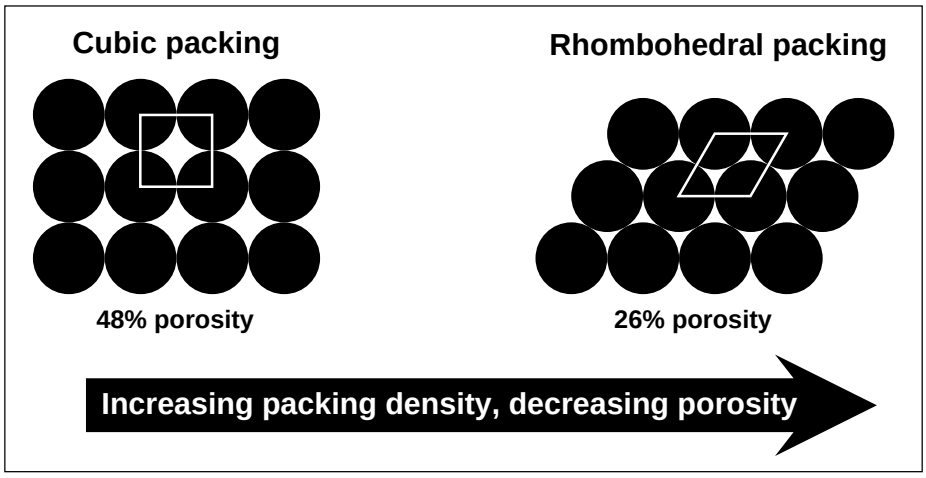

Figure 2-22. End-member styles of packing of spheres of equal diameter and their associated porosities.

spherical. In nature, angular grains tend to support a looser packing arrangement (with larger porosity) than rounded grains.

Grain Size

By itself, grain size has no direct effect on the porosity of sediment. For example, for a sediment composed of equant spheres with cubic packing it can be shown that Eq. 2-25 reduces to

$$P = (1 - \frac{\pi}{6}) \times 100 \qquad \text{Eq. 2-26}$$

and is, therefore, constant (P = 48%) and clearly independent of grain size.

Indirectly grain size may have some influence on porosity. For example, packing of a sediment tends to increase with the settling velocity of the particles. When relatively larger particles, with high settling velocities, impact on a substrate they tend to jostle the previously-deposited grains into tighter packing (with lower porosity).

Several studies have shown various relationships between grain size and porosity that could be explained in terms of other factors. In unconsolidated sands porosity tends to increase as grain size decreases. This is because the finer sand tends to be more angular than coarse sand and, therefore, will support a more open packing. In sandstones the opposite trend has been recognized: porosity tends to increase with increasing grain size. This outcome is due to the greater tendency of fine sand to lose volume when compacted upon burial (see below) compared to the lower compaction of coarse sand. Thus, the conflicting apparent relationships between grain size and porosity are due to factors other than grain size.

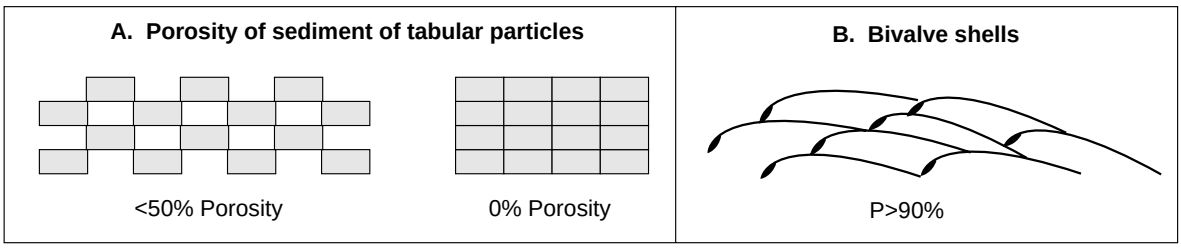

Figure 2-23. Influence of particle shape on packing and porosity.

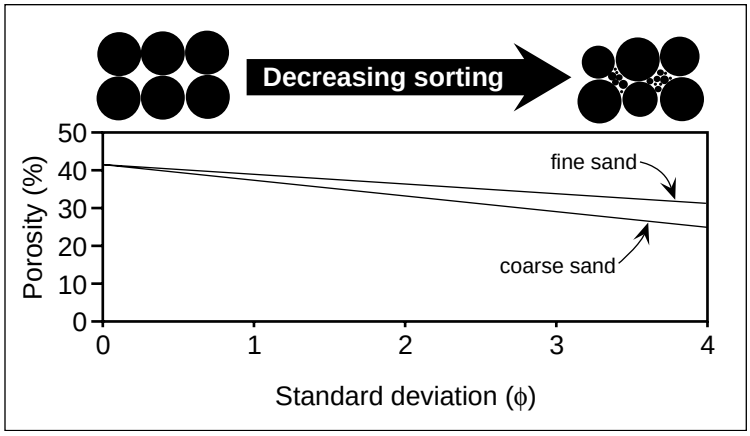

Figure 2-24. Schematic illustration showing the relationship between sorting and porosity in clay-free sands. Based on data from Nagtegaal (1978) and Beard and Weyl (1973).

Sorting

The relationship between sorting and porosity is fairly straight-forward: as sorting becomes poorer (i.e., the standard deviation of the grain size distribution increases) porosity decreases. This is illustrated in figure 2-24 for the case of **clay-free** sand. The reason for this relationship is obvious: the poorer the sorting the wider range of grain sizes within the sediment and the greater likelihood of finer grains filling the void spaces between larger grains. What is perhaps less obvious is the reason for the differences in the curves for fine and coarse sand (Fig. 2-24). Note that the minimum porosity for fine sand is greater than the minimum porosity for coarse sand. This is because a poorly sorted coarse sand has an abundance of fine material to clog the large pore spaces between the coarse grains. However, a poorly sorted fine sand which is free of clay (as in the case of the curves shown above) the poor sorting is by virtue of the presence of coarser sands that will not clog the pores of the finer sand. A similar difference in minimum sorting **would not** be expected if clay were available to clog the pores of the fine sand. Indeed, the presence of clays tends to significantly reduce the porosity of sediment.

Post-burial Processes

Several different processes act in conjunction to alter porosity after a sediment has been buried due to subsequent sedimentation on the overlying depositional surface. Figure 2-25 shows the typical reduction of porosity of sands with burial (although the forms of such curves vary) that can be explained by the processes summarized below. Note that some post-burial processes cause an increase in porosity; such porosity is refered to as **secondary porosity**. The expression **Primary granular porosity** is often used to distinguish porosity due to the character of the sediment prior to burial from porosity due to changes after burial.

Compaction—With burial the weight of overlying sediment may force the sediment into a tighter packing, thereby reducing its porosity. Quartz sand shows little response to compaction; experiments have reduced the porosity of quartz sand by only a few percent due to rearrangement and breakage under stress. The reduction in porosity with compaction increases with increasing proportions of ductile (deformable) particles, especially clays minerals. When first deposited, some muds (composed largely of clays) have a very high porosity (in excess of 70%) but compaction with burial under a thousand metres of sediment reduces that porosity to 5 to 10%.

Cementation—The precipitation of cements within a sediment may begin almost immediately following deposition or make take place after millions of years and relatively deep burial. The most common cements are calcite and quartz that precipitates out of solution from saturated waters between grains and gradually fills in the previously open void space, potentially reducing porosity to 0%.

Clay formation—Chemical alteration of some minerals, particularly feldspars which are a common constituent of

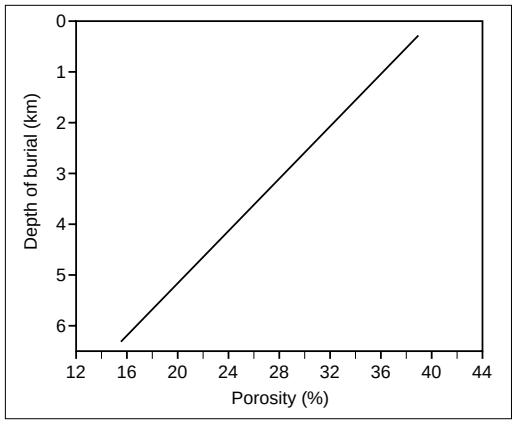

Figure 2-25. Illustration showing the reduction in porosity of tertiary sands in Louisiana. After Blatt, Middleton and Murray (1980).

clastic sediment, results in the formation of very fine-grained clay minerals that tend to accumulate within the pore spaces between primary sediment grains. The formation of clays, therefore, may increase the total volume of the rock at the expense of the pore volume, thereby reducing porosity.

Solution — Waters within and passing through sediment and sedimentary rocks may not precipitate cements. If the waters are undersaturated with respect to the minerals with which they are in contact, these waters may dissolve the sediment grains, leaving a cavity or vug where there had once been solid rock (note that the vugs can range from microscopic in size to the size of caverns). Such solution increases the total void space at the expense of the total rock volume; i.e., it increases the porosity. The additional void space produced by solution is termed **secondary porosity**. Carbonate rocks (which are relatively soluble) are particularly prone to the development of secondary porosity by solution.

Pressure solution is a process that can cause a reduction in porosity following burial when mineral grains begin to dissolve at the grain contacts (Fig.2-26). Minerals under stress solution tend to dissolve more readily than unstressed minerals. Within a sediment the weight of overlying material is transferred between particles at the points where they are in contact. At the contacts the pressures can be immense and solution may occur as long as there is fluid within the adjacent pore spaces. The tangential contacts between grains become increasingly flat as material is removed into solution. The boundary between grains that have undergone pressure solution is said to be **sutured**. As the grains lose material at their contacts the pore space becomes markedly shorter and its volume is reduced. Concurrent with pressure solution insoluble material may accumulate in the pore space along with cements. Combined, the reduction of pore length and the deposition of material in the remaining space can cause a dramatic reduction in pore space. Once again, carbonate rocks are most prone to pressure solution and it has been documented to occur at burial depths of only a few tens of metres. Modern carbonate sediment has porosities ranging from 40 to 80% but carbonate rocks rarely have porosities larger than 15%. Much of this reduction can be attributed to pressure solution. Siliciclastic sedimentary rocks can also undergo pressure solution but this is much less effective in reducing porosity than in carbonates.

Fracturing — Fracturing of any rock, sedimentary or otherwise, will lead to an increase in porosity. Such additional porosity contributes to the secondary porosity of a rock. Fracture porosity may be especially important in rocks in which primary granular porosity is not well preserved.

Permeability (Darcy's Law)

Permeability (k) is related to the ability of a fluid (liquid or gas) to flow through any porous substance (e.g., a sediment). It was first defined by the French hydrologist Henri Darcy in 1851. Figure 2-27 very schematically illustrates how permeability is defined. Darcy's Law (Eq. 2-27) is an empirical formula that predicts the rate of flow of fluid through a sediment. It can be used to experimentally determine permeability by measuring the rate of

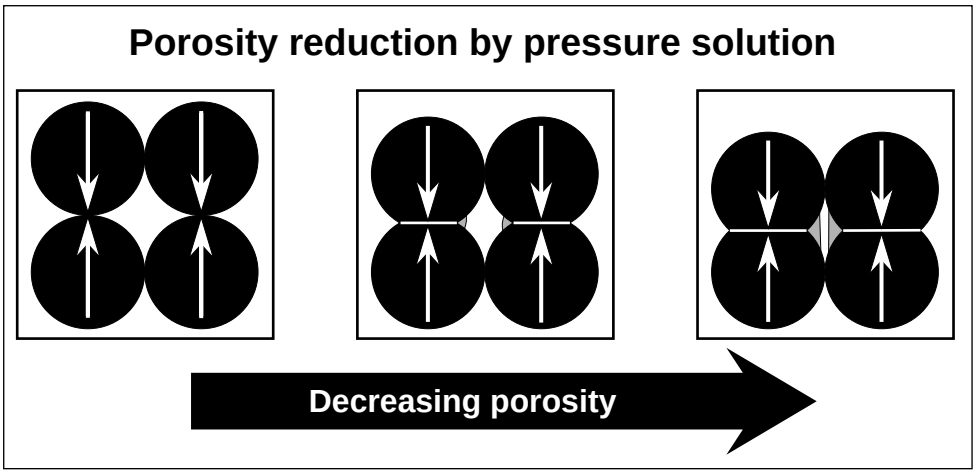

Figure 2-26. Schematic illustration showing the reduction in porosity due to pressure.

discharge of fluid of known viscosity through a specimen under a known pressure gradient and solving for *k* in Eq. 6-3. Note that *k* is just an empirical constant, that depends on conditions within the rock , but one which has an important physical interpretation (termed permeability).

Darcy's Law: $$Q = k\frac{A\Delta p}{\mu L}$$ Eq. 2-27

The terms are defined in figure 2-27.

For the sake of simplicity we will re-arrange the formula as follows:

$$\frac{Q}{A} = k \times \frac{1}{\mu} \times \frac{\Delta p}{L}$$ Eq. 2-28

Q/A is equal to the average (apparent) velocity (V, in cm s^{-1}) at which the fluid is being discharged from the sediment. Assuming that there is no compression of the fluid this is also the average velocity at which the fluid will pass through the sediment. Eq. 2-28 may be re-written:

$$V = k \times \frac{1}{\mu} \times \frac{\Delta p}{L}$$ Eq. 2-29

Beginning with the right-hand-side of this formula, Δ/L is the pressure gradient along the distance of flow and

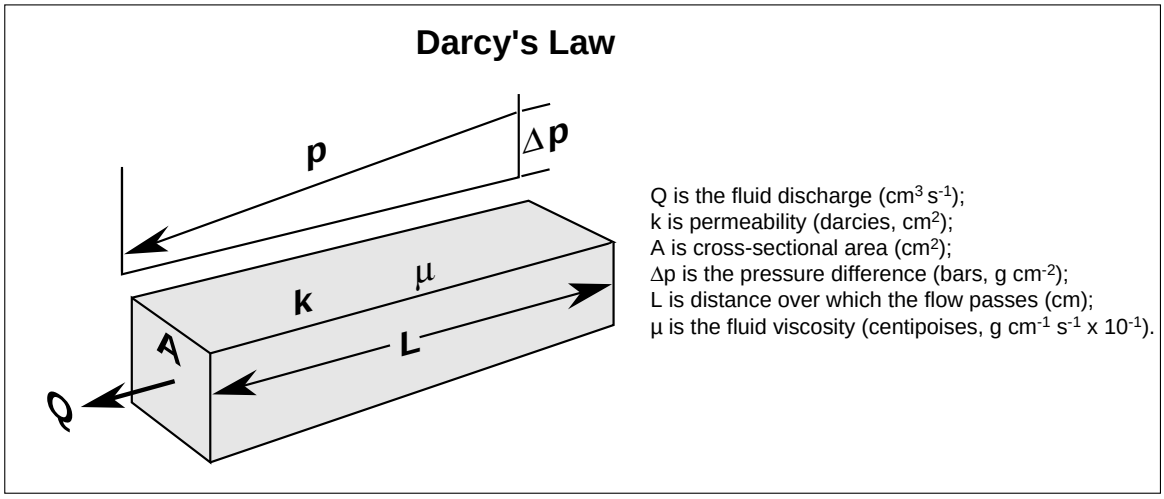

Figure 2-27. Schematic illustration defining Darcy's equation. See text for discussion.

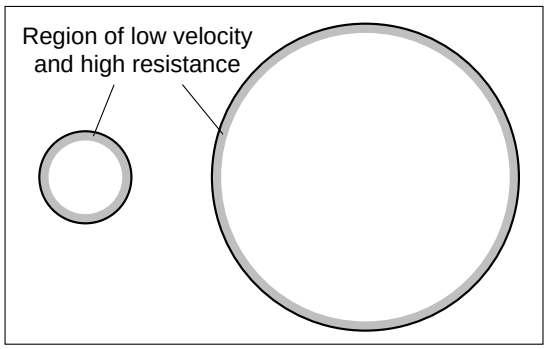

Figure 2-28. The relationship between the cross-sectional area of a pathway and the relative proportion of that cross-sectional area where fluid velocity is small due to viscous resistance along the wall of the pathway.

represents the force that is acting to push the fluid through the sediment. As the pressure gradient increases so will the average velocity. The term $1/\mu$ is a measure of how easily the fluid can flow through the sediment (i.e., as viscosity, a measure of fluid resistance to deformation, increases, $1/\mu$ decreases). Therefore, as viscosity increases the velocity must decrease. So the velocity of a fluid passing through a sediment depends on the force applied to that fluid and on how much the fluid will resist flow through the sediment. But we have not yet considered how the sediment itself will influence the velocity of the fluid passing though it; that is the role of the permeability term in the Darcy's Law. Permeability is a measure of how the pathway(s) through the sediment will affect the resistance of the flow of fluid; that is, it is related to the average diameter and total length of the pathways. Certainly if the "holes" or "pathways" through the sediment are small it will be more difficult to push the fluid through than if the holes are large. This is because the greatest viscous resistance to flow occurs along the walls of the pathway; the smaller the diameter of the pathway the greater the viscous resistance. This is illustrated in figure 2-28 which shows that for a pathway with a small cross-sectional area the region close to the wall of the pathway, where flow velocity is low due to viscous resistance, will be a relatively large proportion of the total cross-sectional area of the pathway. Conversely, when the cross-sectional area is large the region of low velocity will be relatively small compared to the total cross-sectional area of the pathway. Because k has units of cm^2 (this is required to make the equation dimensionally correct) it is useful to think of permeability as some measure of the cross-sectional area of the pathways through which the fluid flows. Therefore, all other things being equal, a large pathway with large cross-sectional area (i.e., k is large) will allow fluid to move at a higher average velocity, in response to a given pressure, than will a smaller pathway (k is small) with fluid under the same pressure. Of course, the pathways through a sediment are very variable in size so that permeability should be thought of as some *average cross-sectional area* for the entire network of pathways through a sediment. This is a simplistic but useful view of permeability. The total viscous resistance will also vary with the total distance that the fluid must pass along the pathways; thus, permeability also varies inversely with the **tortuosity** of the pathways. In this context tortuosity is a measure of the degree of deviation of a pathway from a straight line; the more irregular the pathway the greater the tortuosity (Fig. 2-29). Thus, the larger the tortuosity of the pathways through a rock the lower the permeability. Again, this is related to the degree of resistance to flow that is due to the total character of the pathway.

The units of permeability are termed **darcies** (d) and have dimensions of cm^2. However, the permeability of many rocks is much less than 1 darcy so that it is commonly expressed in terms of millidarcies (md; 1/1000 of a darcy). As originally defined, 1 darcy is the permeability which allows a fluid of one centipoise viscosity to flow

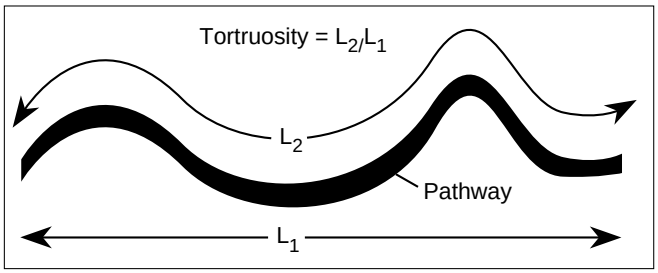

Figure 2-29. Definition of tortuosity. See text for discussion.

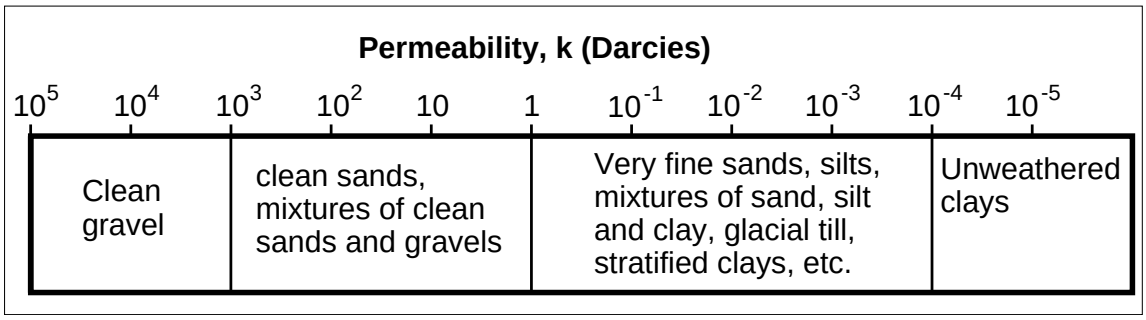

Figure 2-30. Values of permeability of **unconsolidated** sediments. After Pettijohn, Potter and Siever, 1973.

at one centimetre per second, given a pressure gradient of one atmosphere per centimetre. Figure 2-30 shows the range of permeability of unconsolidated sediment.

Controls on Permeability

It should be obvious from the above discussion that any property of a sediment that controls the size of the pore spaces and/or the tortuosity of the pathways will control the permeability. These are much the same as the controls on porosity, with a few notable exceptions.

Porosity & Packing

Figure 2-31A schematically shows the general relationship between porosity and permeability. Permeability tends to increase with increasing intergranular porosity. The reason for this should be made clear by re-examining figure 2-22: the tighter the packing (and the lower the intergranular porosity) the smaller the "pathways" through which a fluid will move and the lower the permeability of the sediment. Therefore a sediment of a given size with cubic packing will have a higher permeability than a sediment of the same size with rhombohedral packing. However, many rocks (especially shales and some carbonates, particularly those with secondary porosity formed by solution) may have high porosity but low permeability. This occurs when the pore spaces are not well interconnected and the "average" pathway size is very small. Conversely, the presence of fractures in rocks may significantly increase the permeability while increasing the porosity only slightly. A fracture of 0.25 mm width. in a rock will allow the passage of fluid at a rate equal to that passing through 13.5 metres of unfractured rock with a uniform permeability of 100 md. The relatively large permeability along fractures is due to a combination of their size, compared to the pore spaces of many rocks, and also because they are especially well-connected. Thus a rock with very low porosity may have very high permeability if it is extensively fractured.

Grain Size and Sorting

Unlike porosity, permeability varies with the grain size of the sediment. This arises from the fact that, in addition to packing, the size of the pores between grains is determined by grain size. To illustrate the relationship between grain size and pore area consider a sediment of uniform spheres with cubic packing (see Fig. 2-22). It can be shown that the average pore area (P_A) is related to sphere diameter (d) by:

$$P_A = 0.74\, d^2 \qquad \text{Eq. 2-30}$$

Figure 2-32 illustrates the graph of the solution to Eq. 2-30 and shows how pore area increases with increasing grain size. Because the pore spaces form the pathways for fluid flow, the permeability of the sediment varies in a similar manner: as grain size increases so does the size of the connected pores (although the total pore volume remains unchanged) so that, all other factors being constant, and permeability also increases. This tendency also is shown

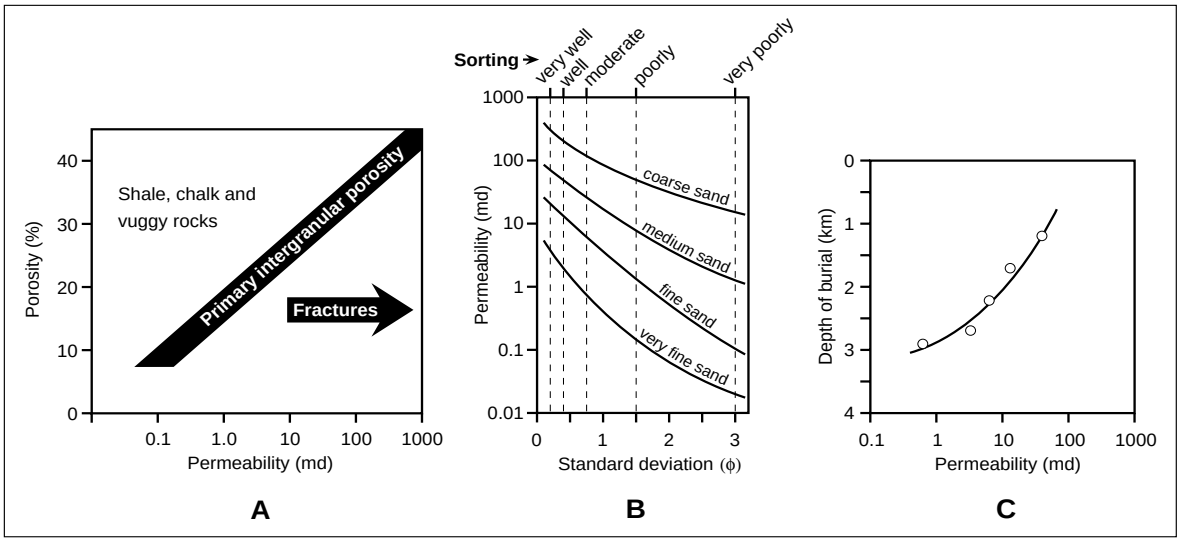

Figure 2-31. A. Schematic illustration showing the relationship between porosity and permeability (after Selley, 1982). B. Illustration showing the effect of grain size and sorting on the permeability of clay-free, unconsolidated sands (based on data from Nagtegaal, 1978 and Beard and Weyl, 1973). C. A graph showing the reduction of permeability with burial based on data from the Ventura Oil Field, California (based on data from Hsü, 1977).

for natural sands in figure 2-31B.

The sorting of a sediment will have an obvious effect on its permeability. Well-sorted sands will have open pore spaces and, therefore, high permeability. As sorting becomes poorer the finer fraction will tend to clog pores (i.e., reduce their average area) and pathways so as to retard the flow of fluid, thereby reducing permeability. Figure 2-31B shows that sorting may cause permeability to vary over several orders of magnitude in sediment of the same mean size.

Post-burial Processes

Like porosity, processes acting after burial of a sediment can have a considerable influence on permeability. Figure 2-31C shows an example of the typical decrease in permeability that occurs with increasing burial depth.

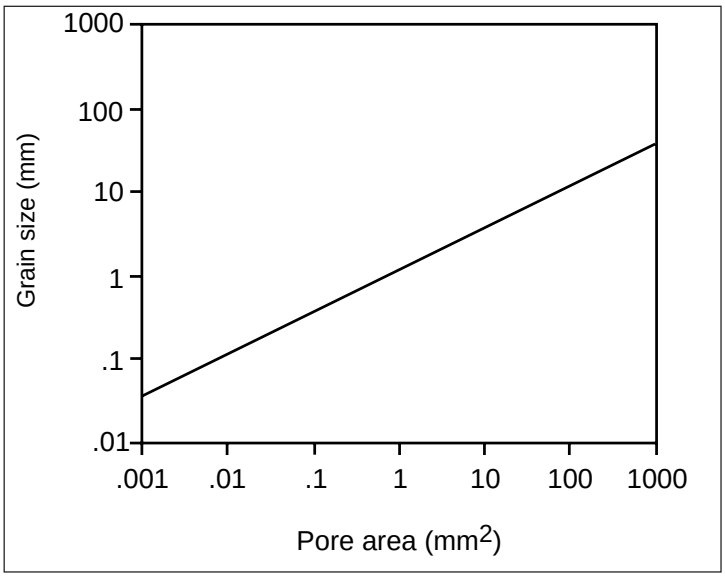

Figure 2-32. Relationship between grain diameter and average pore area for spheres with cubic packing. Curve graphically illustrates solutions to Eq. 2-30.

Compaction, cementation, pressure solution, and formation of clay minerals all act to reduce the permeability of a rock by reducing the size of pore spaces and by increasing the tortuosity of the pathways. As noted above, however, fracturing can increase permeability immensely. Also, solution along pathways may enhance permeability.

Directional Variation of Permeability

An important attribute of the permeability of many rocks is that it may vary with direction. Such anisotropic (not equal in all directions) permeability is particularly notable in bedded sediment where permeability is generally greatest along planes parallel (or at a slight angle) to bedding. The presence of bedding usually reflects some variation in grain size through a package of sedimentary rock. Layers of fine sediment bounding coarser layers will impede permeability in the direction perpendicular to bedding and fluid will flow most easily through the coarser layers, parallel to the plane of bedding. Permeability may also be larger in a given direction along the plane parallel to bedding. When elongated grains are abundant in a deposit they commonly have a preferred orientation and fluids moving through the sediment will receive least resistance along the direction parallel to the grain axes. Fractures in rocks commonly develop with a preferred strike direction and permeability will be greatly enhanced in the direction parallel to strike.

GRAIN ORIENTATION

Introduction

In sedimentology the term **fabric** refers to all aspects of the spatial arrangement of particles in a sediment and includes both packing (which was dealt with in the previous section) and grain orientation. However, in practice, the term has come to refer principally to the orientation of grains (this practice may have been inherited from metamorphic geology). Grain orientation is one of the fundamental sediment properties and should be included in any complete description of an *in situ* sediment or sedimentary rock. It may influence other properties such as permeability; therefore, grain orientation may be an important consideration in predicting the direction of movement of contaminant through a sediment.

Grain orientation is a potentially powerful tool for the interpretation of processes that acted on a sediment at the time of deposition. As we have seen, other sediment properties have been of limited value in interpreting sedimentary processes. Both grain size distribution and grain shape may reflect something of the processes in the depositional environment but both may also preserve characteristics inherited from the source material that produced the sediment. In contrast, grain orientation is determined at the time that the sediment was deposited; it inherits no attribute from its source material. Once a particle has attained a preferred orientation at the time of deposition it remains constant unless: (1) it is modified by compaction, a trivial concern in sand-size sediment; (2) it is modified by post-depositional disturbance: soft-sediment deformation or bioturbation (both relatively easily recognized); (3) it is modified by tectonic deformation (shearing and folding by tectonic processes). This section of these notes describes the nature of grain orientation, how directional data are graphically displayed and treated statistically, and how such data may be used to infer processes that acted in ancient depositional environments.

Measuring grain orientation

The orientation of a grain is determined by measuring the directional attributes of the long (a-axis) and intermediate (b-axis) axes of particles. In gravel-size sediment we may use a compass to directly measure the trend of a clasts a-axis and the strike and dip of its a-b plane (Fig.2-33), with respect to the plane of the surface on which the particle lies. The angle of dip of the a-b plane is termed the imbrication angle and the direction of dip is termed the **imbrication direction** of the clast and such a dipping clast is said to be imbricate. From studies of modern sediment it is well known that particles tend to be imbricate into the flow (i.e., the imbrication direction points in the up-current direction).

In sand-size sediment the orientations of the apparent axes are measured in thin sections but such measurements are generally limited to grains with apparent length to width ratios of 3:2 (this ensures that the true

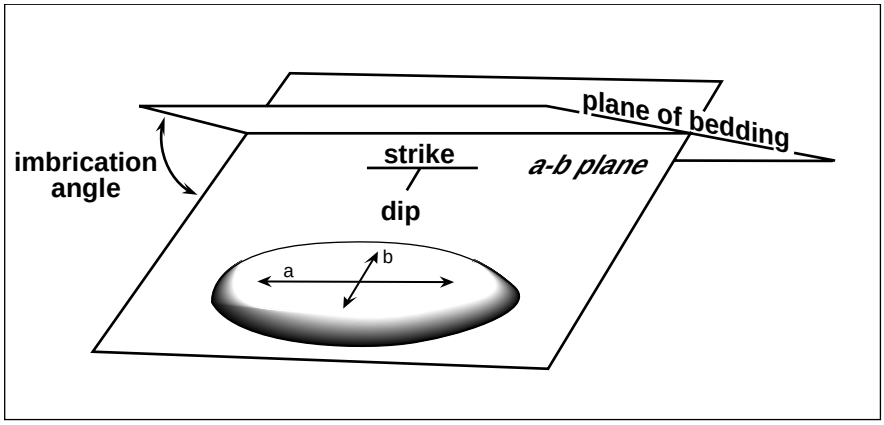

Figure 2-33. Illustration showing the directional attributes of gravel size sediment that are commonly measured in outcrop. Note that the a-b plane is the plane passing through the clast such that the surface defined by the intersection of the clast and the plane has the maximum possible area (i.e., the a-b plane is the maximum projection plane) and that the c-axis of the particle is orthogonal to the a-b plane. In practice, for such a clast we measure the trend of the a-axis, the strike of the a-b plane and its dip direction, which is at 90° to the strike, and angle; termed the imbrication direction and angle, respectively).

longest axis is measured; when grains have lower ratios it is difficult to distinguish the length from the width). Note that for the measured directions of axes to be of any value the orientation of the specimen in its original position in outcrop must be marked directly on the specimen; aspects of the original orientation include: direction to top, direction to north, the plane of bedding seen in outcrop and the horizontal plane. It is particularly important to note the orientation of the plane of bedding because grains will have been aligned on their depositional surface, the same surface that controls the geometry of bedding . The trends of the apparent a-axes are measured on thin sections cut in the plane parallel to bedding in a specimen of sediment or rock. The imbrication direction is determined from thin sections cut in the vertical plane (normal to bedding). The determination of imbrication direction must be made on the basis of two thin sections: one in the vertical plane that is parallel to the mean long axis trend, as measured on the bedding plane, the other in the vertical plane trending normal to the mean long axis trend. The reasons for this will become apparent in the following section.

Types of grain fabric

The grain fabric of a sediment, determined by either method described above, may be classified into two broad groups: isotropic fabric and anisotropic fabric. The latter may be further classified according to the specific directional attributes of the particles.

Isotropic fabric

A sediment that displays no preferred alignment of grains is said to have an **isotropic** fabric (i.e., grain orientation varies uniformly and displays no preferred alignment of particles; syn. disorganized fabric; Fig. 2-34). Such a fabric will appear the same in every plane through a specimen. Any sediment that consists of particles with a high sphericity will appear isotropic for the simple reason that it is not possible to measure axes orientations (Fig. 2-34A). In sediment of non-spherical particles (Fig. 2-34B) such fabrics may be primary (i.e., developed at the time of deposition) or result from reworking of the sediment by burrowing organisms.

Anisotropic fabric

Any sediment that displays a preferred alignment of particles in any direction and in any plane is said to have an **anisotropic** fabric (i.e., **not** equal in all directions). Figure 2-35 shows the two common forms of anisotropic fabric that develop in sand and gravel.

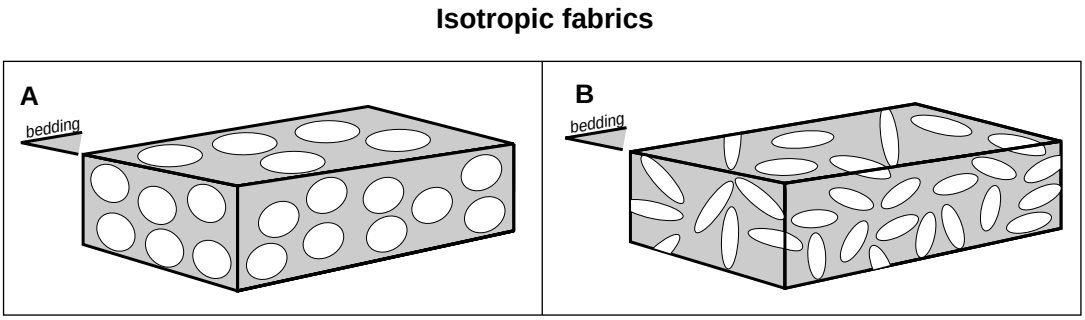

Figure 2-34. A. Isotropic fabric in a sediment made up of spherical particles. B. Isotropic fabric due to random alignment of grains.

a-axis transverse, b-axis imbricate [a(t) b(i)]

The particle shown in figure 2-33 has this orientation. Figure 2-35A also shows this fabric as it would be seen in three orthogonal planes through a sediment or sedimentary rock. From studies of modern sediment, where current directions are known, we recognize this style of fabric as being characterized by a-axes (seen on the plane of the depositional surface; shown as the bedding plane in Fig. 2-35A and B) that are aligned transverse to the current direction. Imbrication of the a-b plane is up-current (i.e., into the flow) and the direction of imbrication is along the trend of the b-axis. Hence, the shorthand notation: a(t) b(i) - a-axis transverse to flow and b-axis imbricate. Note that the grains appear horizontal in the vertical plane parallel to a-axes on bedding.

a-axis parallel, a-axis imbricate [a(p) a(i)]

This fabric is shown in figure 2-35B. In this case the a-axis of each grain is aligned parallel to the current and the a-b plane is imbricate into the flow; the imbrication direction is along the trend of the a-axis. The shorthand notation for this fabric is a(p) a(i): a-axis parallel to flow and a-axis imbricate. The mean trend of grains seen in the vertical plane aligned normal to a-axes is essentially parallel to bedding or nearly horizontal.

Complex anisotropic fabric

Some sediment displays an equal or unequal mixture of a(t) b(i) and a(p) a(i) fabrics. Such sediment has a complex fabric that may be difficult to distinguish from an isotropic fabric.

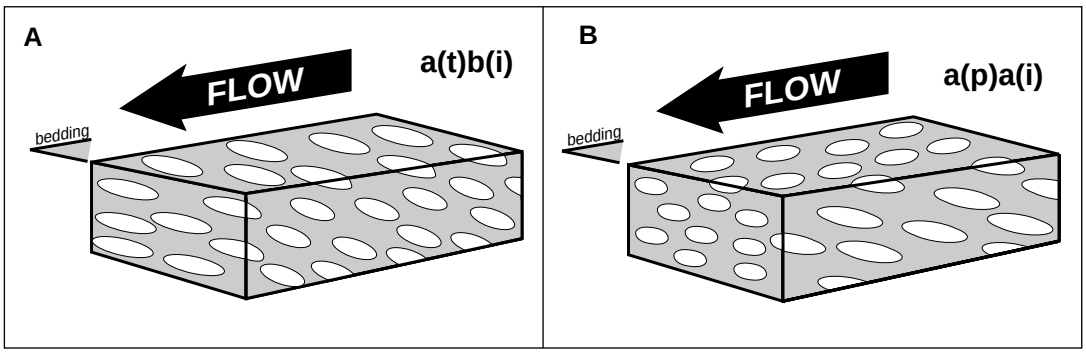

Figure 2-35. Schematic illustration showing examples of anisotropic fabric. A. Grain a-axes are aligned transverse to flow and b-axes dip into the flow. B. Grain a-axes are aligned parallel to and dip into the flow. See text for further explanation.

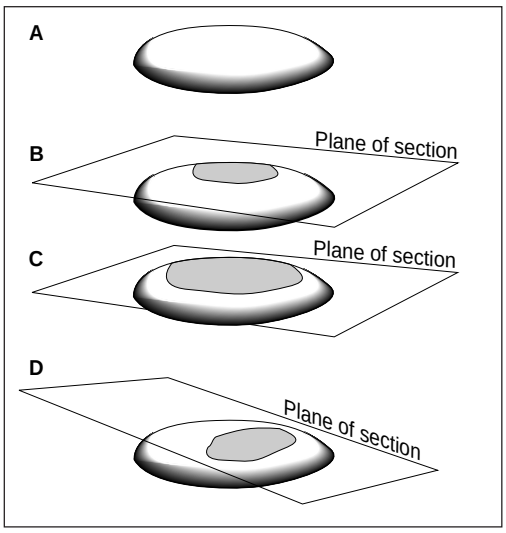

Figure 2-36. Illustration showing the relationship between apparent axes lengths and orientation due to the position of the plane of section. A. A three-dimensional sketch of a particle as viewed at an angle to its a-b plane. B. Shaded area shows the form and area of the grain at its intersection with a plane (termed the plane of section) that is parallel to the a-b plane, but well above the a-b plane. Note the reduction of axes lengths in the image seen on the plane of section. C. Shaded area shows a larger form and area than in B as the plane of the section moves nearer to the a-b plane of the grain. Note that true axes lengths will be seen only if the plane of the section is in the a-b plane of the particle. D. Shaded area shows the form of a grain in section oblique to the a-b plane of the particle. Note that apparent axes (on the shaded area) are not parallel to the true axes of the grain. Similar distortion arises when grains have variable orientation with respect to a fixed plane of section.

The problem with measuring grain orientation on sections

Take a close look at figure 2-35 (A and B) and consider how the angular relationship between the grain and the plane of view will influence the apparent axes lengths and orientations. In figure 2-35A, on the plane of bedding, we see the a-axes lengths but the b-axes lengths are shortened by an amount that depends on the angle of imbrication (the steeper the angle the shorter the apparent b-axis; if the grains were vertical we would see the c-axes on that plane). In the plane that is vertical to bedding and transverse to the trend of a-axes we see the form of the grain that is defined by the b-c plane. In the vertical plane that trends parallel to the long axes on the bedding-parallel plane we see the form of grains that is defined by the a-c plane (actually the apparent c-axis will exceed the true c-axis length as the angle of imbrication increases; if the grains were vertical we would see the b-axis on this plane). This illustrates the problem that the two dimensional view of a three dimensional object depends on the angular relationship between the directional attributes of the object and the orientation of the plane of view.

In thin sections cut from rocks this problem is compounded by the fact that we have little control over where the plane of view will intersect the grains. The control on apparent axes lengths by the plane of intersection of the surface with the grain is shown in figure 2-36B and C. Figure 2-36D shows how the angular relationship between a grain and the plane of section will affect not only its apparent axes lengths but also their orientations. Specifically, if the plane of view is not in and parallel to the a-b plane of the particle we will see a distorted form of the grain. Thus, we have a considerable error in measuring grain orientation in rocks consisting of sand-size sediment. This is minimized if care is taken to prepare the first section in the plane of bedding (a known surface with a predictable relationship to the orientation of the grains). Also, because the angle at which the grains dip below the bedding surface is relatively small (averaging up to approximately 25°) the distortion of form and orientation is relatively small. Finally, when collecting such data we must ensure that a large enough number of grains are measured to balance out such error (i.e., normally in excess of 100 grains must be measured but this number will vary depending on the amount of true variation in grain orientations). It should be clear from this that when such data are described it is very important to make it clear that data are based on measurements made on **apparent** axes, not true axes; all such data collected from thin sections have this limitation. In all remaining figures that deal with grain orientation in this chapter only data on apparent axes are reported.

Displaying directional data

Grain orientation is just one of a large number of types of directional data that may be gathered by a sedimentologist (well see others through the course of these notes). When such data have been compiled they must be displayed to recognize, at least visually, any significant directional trends that may be interpreted. For

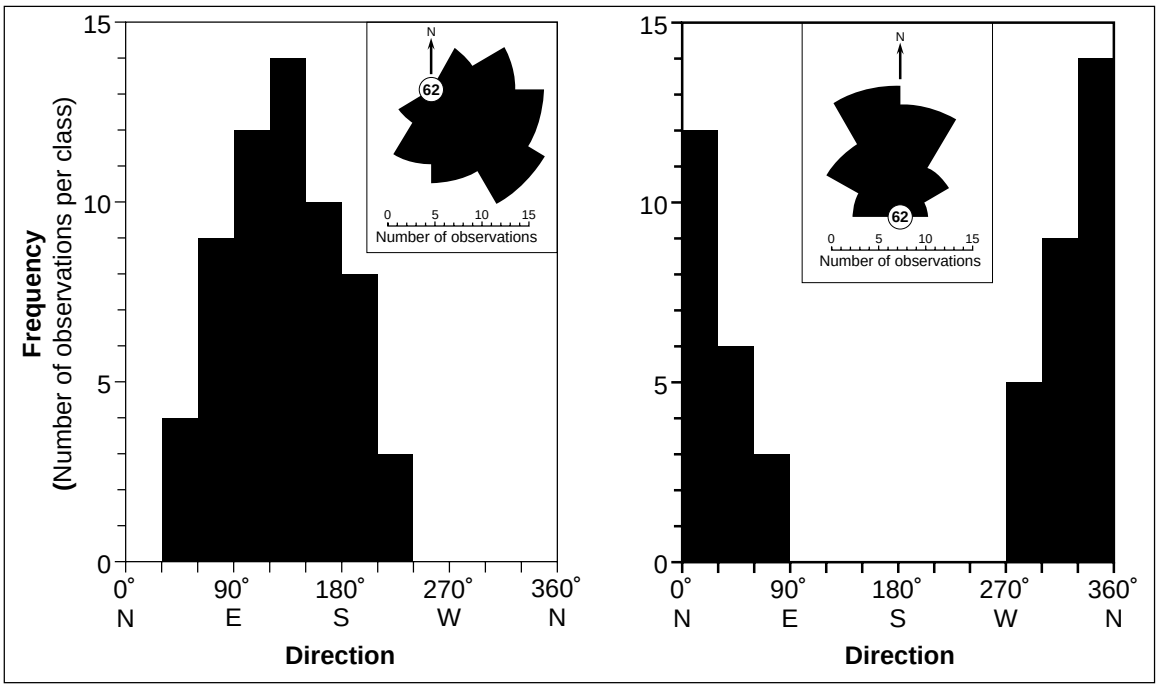

Figure 2-37. Examples of directional data plotted as conventional histograms and as rose diagrams (inset).

example, if we have a set of measurements of the imbrication direction of a number of particles we will need to determine whether the data are consistent and what is the mean imbrication direction. The imbrication direction will indicate the upstream direction with respect to the current that deposited the sediment. If such deposits contain fine gold particles we might want to know where the sediment came from so that we might find its source; the imbrication direction will point towards that source. Statistical treatment of directional data will be considered in the next section.

Sedimentologists display directional data on a form of circular histogram that is commonly referred to as a **rose diagram**. Consider the directional data plotted in the form of an ordinary histogram in figure 2-37A. The number of measurements (i.e., the frequency) in 30° classes is shown over the range 0 to 360° (a full circle; north is generally taken to be towards 0°). You can see from this histogram that the modal direction is in the range 120-149° (the southeast) and the data varies almost symmetrically about that mode. Inset in figure 2-37A is a rose diagram for the same data and it shows the same trend. However, it is obviously easier to visualize the directional significance of the data plotted on the rose diagram. Figure 2-37B shows another set of data plotted on a regular histogram and a rose diagram. In this case we can recognize two prominent modes, one from 0 to 29° and another from 330 to 359°. It is not readily apparent how these two modes are related until we look at the form of the rose diagram (inset in Fig. 2-37B). The rose diagram more clearly shows the overall trend of the directional data (in this case pointing towards the north-northwest). The visual impact of a rose diagram is important when we compare different data sets and particularly when we plot such diagrams on maps.

Figure 2-38 illustrates how rose diagrams are constructed using the example of data describing imbrication direction. The class intervals define the angle of curvature of pie-shaped segments that have a length equal to the number (this may be expressed as a percentage) of observations per class (i.e., the frequency per class). In figure 2-38 the class interval is 30° and the scale of frequency is shown radiating from the centre of the circle. The centre of a rose diagram is commonly reserved to note the total number of observations used to construct it.

Two forms of rose diagram are shown in figure 2-38 based on the data given in the table. In rose A the distance (L) from the centre of the circle to each value representing the number of observations per class (N) is equal to the

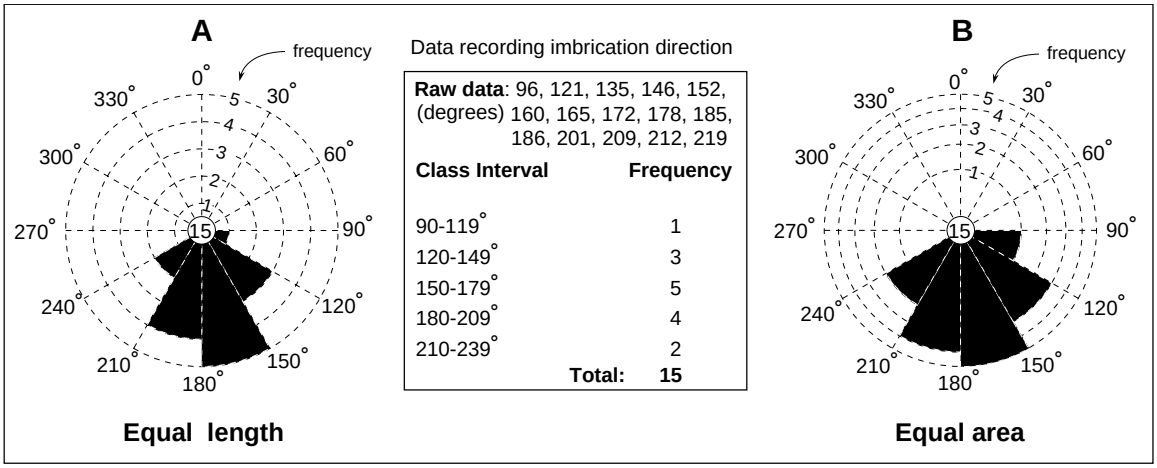

Figure 2-38. Illustration showing the construction of a rose diagram. See text for explanation.

value itself; that is L = N in whatever units you like; the distance between each value on the frequency scale is equal. Thus, a segment of the rose corresponding to a class containing 5 observations is five times longer (extending outward from the origin) than a segment corresponding to a class containing only 1 observation. Rose B shows another frequency scale that many argue is more appropriate. In the case of Rose B the distance from the centre of the circle to any value is given by $L = N^{0.5}$. Therefore, the spacing of the frequency increments decreases outward form the centre of the circle. The reason for this is that in this type of diagram the frequency of observations per class is not shown in terms of the length of the segments but is shown by the relative area of each segment. For example, when such a scale is used the area of a segment of the rose representing 5 observations is equal to five times the area of a segment representing 1 observation. Because rose diagrams are used for their visual impact, some sedimentologists argue that this is a more representative scale than the linear scale. Note the difference in the form of the two roses in figure 2-38. The equal area scale reduces the visual impact of the difference between intervals (compare the relative sizes of the segments corresponding to the 180-209° and 210-239° intervals). All rose diagrams in these notes will be presented with a linear frequency scale.

The form of the rose diagram indicates the directional trends of the data in a visually useful manner. Like any such data, the distribution may have one or more modes and is termed unimodal if one mode is present, bimodal if two modes are present (bipolar if the modes are at 180° to each other) or polymodal if more than two modes are present (Fig. 2-39). Also, the data may vary symmetrically or asymmetrically about the mode(s). The interpretation of the form of a rose will depend on what directional attributes of a sediment have been measured to collect the data. In the case of grain imbrication, the rose points towards the average direction of dip of the a-b planes of the particles and this direction is at 180° to the current that formed the imbrication. Therefore, the rose shown in figure 2-38 shows a mean imbrication direction to the south-southeast, produced by a current flowing towards the north-northwest. Many other directional attributes point in the direction of the current under which they formed and the roses that they produce will point directly in the flow direction.

Many types of directional data are like that shown in figure 2-38 based on grain imbrication; i.e., the imbrication direction is a specific direction determined by the dip of the a-b plane of a particle. However, many features for which directional data may be collected do not point to a specific direction. Consider the long axis orientation of a particle; it does not point in a given direction but rather lies on a directional trend. For example, an a-axis oriented towards 10° has the same orientation as an a-axis oriented towards 190°. Thus, the a-axis of the grain is said to trend along 10-190°. Such directional data are said to be **bidirectional**; pointing in either of two directions which are at 180° to each other. Figure 2-40 shows how such data are commonly dealt with in the construction of rose diagrams. Note that rose diagrams based on bidirectional data are symmetrical with only one side of the rose representing actual measurements and the other side is just its mirror image to give the impression of the bidirectional nature of the data. Figure 2-41 shows the forms of rose diagrams produced by measuring grain

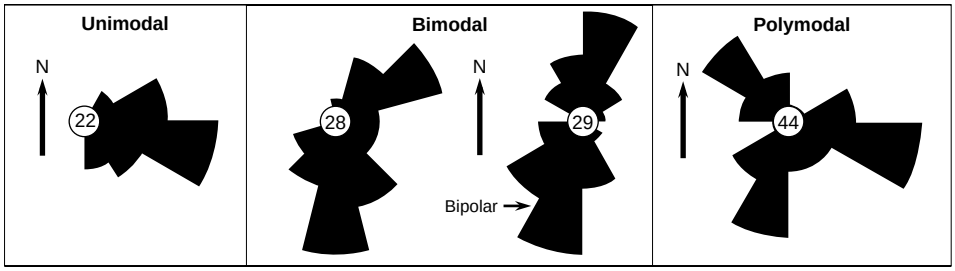

Figure 2-39. Classification of form of rose diagram. After Pettijohn, Potter and Siever, 1973. See text for explanation.

axes orientation in sediment with the anisotropic fabrics described in the previous section. **A word of caution:** be careful to note what is represented by any rose diagram. For example, truly directional data, based on structures produced by tidal currents that flow in directions that vary by 180° over time, may produce essentially symmetrical roses like those shown in figures 2-40 and 2-41.

Statistical treatment of directional data

Normally, directional data are collected in sets of N observations from some particular deposit or associated structure. Like grain size data, a set of directional data will be distributed about some mean direction and will have a range of variation about the mean direction. Unlike grain size data, directional data cannot be treated by regular statistics because each value in a set is a vector quantity and each vector has two components: each observation in a set of directional data will have a direction (θ) and a magnitude (normally each vector has unit magnitude, i.e, its magnitude equals 1; such a vector is termed a unit vector). The descriptive statistics are similar to those applied to scalar quantities (like grain size) but their computation is fundamentally different. Without going into the details of vector algebra this section provides an outline of the various statistics and their implications. The method of summarizing directional data, below, is that of Curray (1956).

For any distribution of directional data the mean is the **resultant vector** (sometimes called the vector mean) formed by summing all of the unit vectors that comprise the data set (e.g., Fig. 2-42). Once again, the resultant vector includes a direction (θ) and a magnitude (R):

$$\bar{\theta} = \tan^{-1}\frac{w}{v} \qquad \text{Eq. 2-31}$$

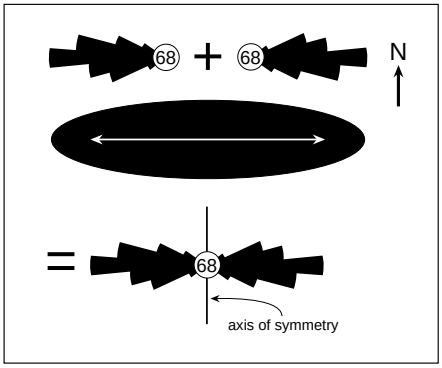

Figure 2-40. Illustration showing the significance of a rose diagram based on bidirectional data. In this case, the rose diagrams represent the long axis orientation of grains seen on a bedding plane; one particle is shown but the roses represent a population of grains with a mean a-axis orientation parallel to that shown on the example particle. Because the a-axis of a particle (like that shown in the illustration) has a trend but no absolute direction, either of the top roses may equally well describe its orientation. However, visually these two roses give two diametrically opposing impressions of the a-axes they represent because they impart a sense of direction to the data; the left-hand rose suggests that the axes point to the west and the right-hand rose suggests that the axes point to the east. To counter this perceived sense of direction it is common practice to construct rose diagrams that are symmetrical, as shown in the lower part of the figure. Note that the lower rose has doubled in size without increasing the number of measurements on which it is based.

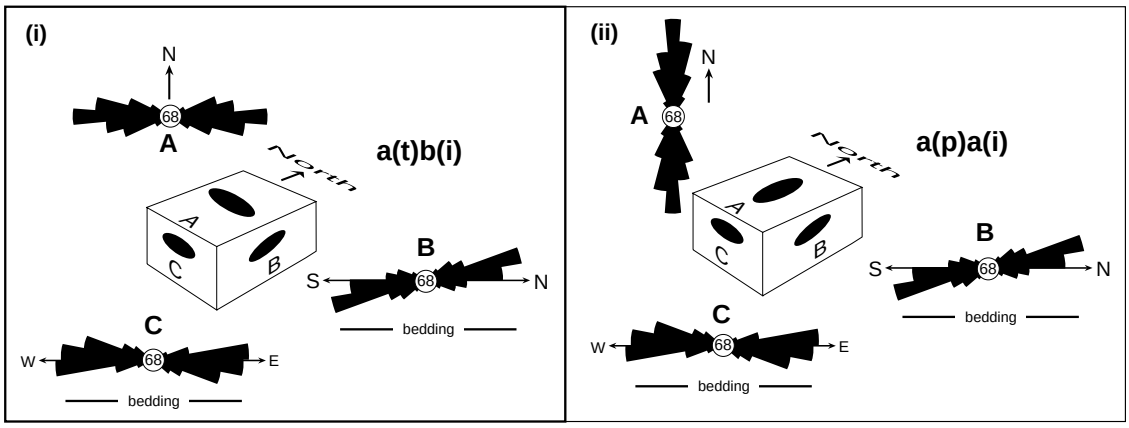

Figure 2-41. Rose diagrams representing two forms of anisotropic fabric (see Fig. 2-35 but note that the blocks shown here are rotated at 180° to the blocks in Fig. 2-35).

Note that $\bar{\theta}$ must be corrected as follows:	if w > 0 and v > 0 then $\bar{\theta}$ = Eq. 2-31; if w > 0 and v < 0 **or** w < 0 and v < 0 then $\bar{\theta}$ = Eq. 2-31 + 180˚; if w < 0 and v > 0 then $\bar{\theta}$ = Eq. 2-31 + 360˚

and

$$R = \sqrt{v^2 + w^2} \qquad \text{Eq. 2-32}$$

where

$$w = \sum_{i=1}^{N \text{ or } NC} n_i \sin \theta_i \qquad \text{Eq. 2-33}$$

and

$$v = \sum_{i=1}^{N \text{ or } NC} n_i \cos \theta_i \qquad \text{Eq. 2-34}$$

and N is the number of observations in the data set. Note that directional data may be treated as either individual measurements (i.e., as raw data) or grouped data (i.e., data are expressed as frequency per class interval). In the case of ungrouped data n_i is equal to 1 (unit magnitude of each vector) and θ_i represents each of the measured directions (from i = 1 to N) of the N vectors in the data set. When data are grouped the quantities above are: n_i is the number of observations in each class interval (from i = 1 to NC) and θ_i is the mid-points of each class interval (from i = 1 to NC) and NC is the number of class intervals (i.e., NC = 360°/CI, where CI is the class interval in degrees).

The magnitude of the resultant vector can also be expressed as a percentage (L) of the total number of

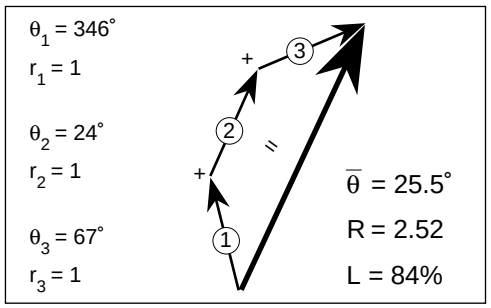

Figure 2-42. Example of the derivation of a resultant vector (syn. vector mean; large arrow) by the summation of unit vectors (small numbered arrows). Each unit vector has the direction shown and a magnitude (r_i) of 1. Use Equations 2-31 to 2-35 to demonstrate the calculation of the direction and magnitude of the resultant vector. Note that the arithmetic mean would be 146° and clearly not representative of the three vectors.

observations (or more specifically, as a percentage of the total length of the unit vectors that comprise the data set):

$$L = \frac{R}{N} \times 100 \qquad \text{Eq. 2-35}$$

The magnitude of the resultant vector, particularly when it is expressed as a L reflects the amount of dispersion of the data (i.e., the degree of variation of directions in the data set). Another, more important, measure of the dispersion of the distribution of directional data is p (defined as the probability that the data are from a population that is uniformly distributed) where:

$$p = e^{-1(L^2 N \times 0.0001)} \qquad \text{Eq. 2-36}$$

p ranges in value from 0 to 1 where p = 0 indicates that there is no chance that the data are uniformly distributed (i.e., the data are from a population that has a preferred orientation) and p = 1 indicates that the data are from a population that is definitely uniformly distributed (i.e., the population has no preferred orientation).

Table 2-4 provides an example of the treatment of directional data, both as ungrouped and grouped data. With a little experience it is possible to acquire some intuition about these statistical properties on the basis of the form of the rose diagram representing a data set.

Interpretation of grain orientation

In the previous section one interpretive use of imbrication direction has already been established; it points in the direction 180° to the direction of the current that acted on the particles. Most workers who have included grain fabric in studies of ancient rocks have used their results to reconstruct **paleoflow** directions. However, there are several other ways in which fabric may be interpreted. To begin with, the anisotropic fabrics can be interpreted in terms of how the particles moved under a flowing current. The a(t)b(i) fabric is produced by currents that roll the particles along the bottom. This is the typical fabric of gravel size sediment; because of their large mass it is difficult to move them in any other way but to roll them along the bottom. In contrast, the a(p)a(i) fabric tends to be the most common fabric in sands and is thought to develop under relatively high rates of deposition and sediment transport and high sediment concentration. Thus, for a given grain size a(p)a(i) fabrics in gravel will be produced under much more energetic currents than those that produce a(t)b(i) fabric. The classic experimental studies of gravel orientation by Johansson (1965, 1976) are required reading for anyone concerned with gravel fabrics. Isotropic fabrics may result from rapid deposition of thick slurries which restrict the independent movement of a particle, hindering the establishment of a preferred orientation.

Figure 2-43 shows an example of a complex anisotropic fabric based on data collected from a sandstone that was deposited in a shallow-marine environment. Two major modes, at 90° to each other, are clearly seen on the rose diagram. This fabric was produced by oscillating currents induced by storm waves in a shallow sea and the bimodality is interpreted in terms of a mixture of transport modes at the time of deposition. The NW-SE mode represents grains with long axes aligned normal to the wave-induced current; these grains were rolled along the bed. The SW-NE mode represents grains that were aligned with their a-axes trending parallel to the current and represent sand that was rapidly deposited from suspension. In this particular case, the bimodality of the fabric reflects processes that act under currents produced by waves and may provide a basis for inferring wave-induced currents in other ancient deposits.

In most sands the imbrication angles of grains range from 5 to 20°, although higher angles have been recorded in sands that are very rapidly deposited by sediment gravity flows. Some research has suggested that imbrication angle may also reflect the power of the current that act to align particles. Experiments by Gupta *et al.* (1987) showed a distinct steepening of imbrication angles with increasingly strong flows. However, recent experiments have shed some doubt on the relationship between imbrication angle and flow strength (Arnott and Hand, 1989).

Results of one recent study have suggested that grain imbrication may be particularly useful in interpreting the nature of transporting currents. Specifically, the results suggested that variation in imbrication angle through

Table 2-4. Example of the statistical treatment of ungrouped and grouped directional data.

Raw data:	184	187	191	196	198	201	204	205
(degrees)	205	207	208	210	212	214	216	222
	224							

Grouped data:

Class Interval	Midpoint	Frequency
180-189°	184.5°	2
190-199°	194.5°	3
200-209°	204.5°	6
210-219°	214.5°	4
220-229°	224.5°	2
	Total:	**17**

Treatment of ungrouped data:

$$w = \sum_{i=1}^{N} n_i \sin\theta_i = -7.04 \qquad v = \sum_{i=1}^{N} n_i \cos\theta_i = -15.13$$

$$\overline{\theta} = \tan^{-1}\frac{-7.04}{-15.13} = 24.95;\ \text{w} < 0 \text{ and v} < 0 \text{ then } \overline{\theta} = \text{Eq.}\,2-31+180^{\text{o}} \ \therefore\ \overline{\theta} = 24.95+180 = 204.95^{\text{o}}$$

$$R = \sqrt{(-15.13)^2 + (-7.04)^2} = 16.69; \qquad L = \frac{16.69}{17}\times 100 = 98.17\%$$

$$p = e^{-1(98.17^2 \times 17 \times 0.0001)} = 7.67\times 10^{-8}$$

Treatment of grouped data:

$$w = \sum_{i=1}^{NC} n_i \sin\theta_i = 2\sin 184.5^{\text{o}} + 3\sin 194.5^{\text{o}} + 6\sin 204.5^{\text{o}} + 4\sin 214.5^{\text{o}} + 2\sin 224.5^{\text{o}} = -7.06$$

$$v = \sum_{i=1}^{NC} n_i \cos\theta_i = 2\cos 184.5^{\text{o}} + 3\cos 194.5^{\text{o}} + 6\cos 204.5^{\text{o}} + 4\cos 214.5^{\text{o}} + 2\cos 224.5^{\text{o}} = -15.08$$

$$\overline{\theta} = \tan^{-1}\frac{-7.06}{-15.08} = 25.09;\ \text{w} < 0 \text{ and v} < 0 \text{ then } \overline{\theta} = \text{Eq.}\,2-31+180^{\text{o}} \ \therefore\ \overline{\theta} = 25.09+180 = 205.09^{\text{o}}$$

$$R = \sqrt{(-15.08)^2 + (-7.06)^2} = 16.65; \qquad L = \frac{16.65}{17}\times 100 = 97.95\%$$

$$p = e^{-1(97.95^2 \times 17 \times 0.0001)} = 8.25\times 10^{-8}$$

Note the slight discrepancy between calculations based on grouped and ungrouped data due to the use of the class mid-points in the case of grouped data.

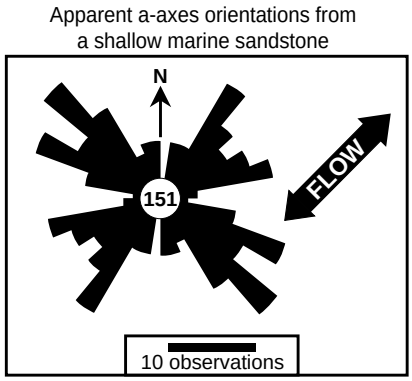

Figure 2-43. An example of a complex anisotropic fabric. Rose diagram shows the trend of apparent long axes seen in the plane parallel to bedding from the Upper Cretaceous Chungo Member (Wapiabi Formation) in the Rocky Mountain Foothills. Note the prominent bimodality of the rose. See text for explanation. After Cheel and Leckie (1992).

a sediment may record changes in current strength and direction over time. Figure 2-44 shows data collected by determining the mean imbrication angle in thin (0.1 to 0.2 mm) vertically contiguous layers through a sediment. In the plots in figure 2-44 each point represents the mean imbrication angle (and direction) in one such layer. The rose diagrams in figure 2-44 are based on all data in the subjacent plot. Figure 2-44 A shows data from the deposits of a river in which currents flowed consistently in the same direction over the course of deposition of the sediment (such currents are said to be "unidirectional"). Within these river deposits the mean imbrication angle is at approximately 13°, dipping into the current. There is little systematic variation in imbrication angle through the deposit, reflecting the constant nature of the flow strength over the period of deposition. For comparison, figure 2-44B shows data from the deposits of a shallow marine setting that was influenced by waves, specifically powerful storm-generated waves. The currents produced by such waves would flow back and forth over 180° over periods on the order of 10 seconds, and are termed oscillatory or "bidirectional" currents. In contrast to the river-formed fabric, the mean imbrication angle is parallel to bedding, reflecting the alternating direction of the current (i.e., the number of grains that are imbricate in one direction are essentially cancelled out by the equal number of grains that are imbricate in the opposing direction). The plot showing variation in imbrication through the shallow marine sandstone is also strikingly different: there is wide variation in imbrication angle and it appears to vary symmetrically about a mean of 0°. Not only is this variation symmetrical, but it is also has a cyclicity that can be proven statistically. The cyclic variation in imbrication angle through the deposit records variation in the magnitude of flow strength under waves: flow strength decreases, from a maximum in one direction, to zero and then increases to a maximum in the opposing direction. Thus, detailed studies of the variation in imbrication angle in sediment may provide a powerful tool in distinguishing the products of unidirectional and oscillatory currents.

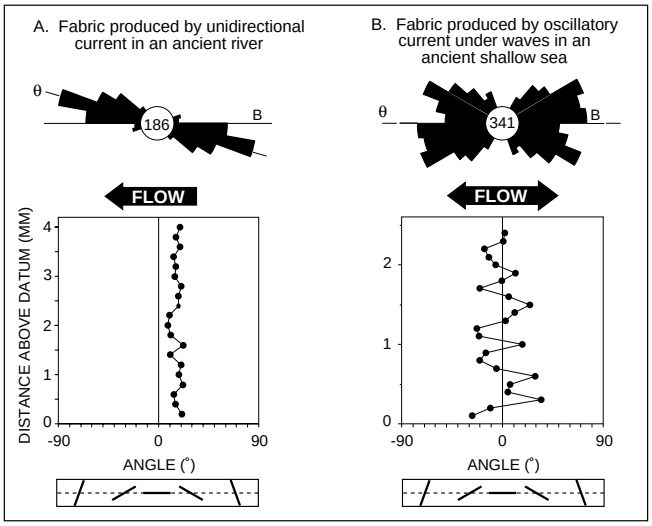

Figure 2-44. Comparison of the fabric of sandstones deposited in fluvial (A) and shallow-marine (B) settings. See text for discussion. After Cheel (1991).